ELSEVIER

A phylogenetic hypothesis for Asilidae based on a total evidence analysis of morphological and DNA sequence data (Insecta: Diptera: Brachycera: Asiloidea)

Torsten Dikow[a,b,1]

[a]*Department of Entomology, Cornell University, Ithaca, NY, USA*
[b]*Division of Invertebrate Zoology, American Museum of Natural History, New York, NY, USA*

Abstract

An hypothesis of phylogenetic relationships of Asilidae and its constituent taxa is presented, combining morphological and DNA sequence data in a total evidence framework. It is based on 77 robber fly species, 11 Asiloidea outgroup species, 211 morphological characters of the adult fly, and approximately 7300 bp of nuclear DNA from five genes (18S and 28S rDNA, *AATS*, *CAD*, and *EF-1α* protein-encoding DNA). The equally weighted, simultaneous parsimony analysis under dynamic homology in POY resulted in a single most parsimonious cladogram with a cost of 27,582 (iterative pass optimization; 27,703 under regular direct optimization). Six of the 12 included subfamily taxa are recovered as monophyletic. Trigonomiminae, previously always considered as monophyletic based on morphology, is shown to be non-monophyletic. Two of the three Trigonomiminae genera, *Holcocephala* Jaennicke, 1867 and *Rhipidocephala* Hermann, 1926, group unexpectedly as the sister taxon to all other Asilidae. Laphriinae, previously seen in the latter position, is the sister group of the remaining Asilidae. Five other subfamily taxa, i.e. Brachyrhopalinae, Dasypogoninae, Stenopogoninae, Tillobromatinae, and Willistonininae, are also shown to be non-monophyletic. The phylogenetic relationships among the higher-level taxa are partly at odds with findings of a recently published morphological study based on more extensive taxon sampling. The total evidence hypothesis is considered as the most informative one, but the respective topologies from the total-evidence, morphology-only, and molecular-only analyses are compared and contrasted in order to discuss the signals from morphological versus molecular data, and to analyze whether the molecular data outcompete the fewer morphological characters. A clade Apioceridae + Mydidae is corroborated as the sister taxon to Asilidae.

© 2009 Gesellschaft für Biologische Systematik. Published by Elsevier GmbH. All rights reserved.

Keywords: Asilidae; Asiloidea; Phylogeny; Total evidence; Dynamic homology; POY

Introduction

Asilidae ('robber flies', 'assassin flies') comprises approximately 7000 described species and therefore is one of the most speciose family taxa among the Diptera or 'true flies' (Asilidae website: http://www.geller-grimm.de/catalog/species.htm). Robber flies are

predatory, generally catching prey insects on the wing; they are distributed worldwide, with the exception of Antarctica. Asilidae have attracted interest from researchers for centuries, primarily due to their generally large adult size and their predatory behavior in the larval and adult life stages, which is unique within Diptera. Recently, nomenclatural and taxonomic studies in the form of updated genus-group taxa (Geller-Grimm 2004) and family-group taxa catalogues (Dikow 2004) have been published. Dikow (2009) has provided a summary of the classificatory history and a comprehensive hypothesis for the phylogeny of higher-level taxa based on 220 morphological characters obtained from 158 species, as well as for the evolutionary relationships of assassin flies to other Asiloidea. Bybee et al. (2004) published the only molecular phylogenetic study on Asilidae to date, based on two mitochondrial and two nuclear genes in 26 species. The present study proposes an hypothesis of phylogenetic relationships of 77 Asilidae species, based on 211 morphological characters of the adult flies and on approximately 7300 bp of DNA sequences from five nuclear genes. The data set is analyzed simultaneously in a total evidence framework.

Total evidence

The publications by Kluge (1989) and Kluge and Wolf (1993) were the first phylogenetic papers to bring the concept of total evidence from the literature on the philosophy of science to phylogenetic systematics (see references in Kluge 1989). Total evidence analysis is defined in these publications as a phylogenetic study simultaneously analyzing all available data; this has also been termed "simultaneous analysis" by Nixon and Carpenter (1996). Total evidence matrices include any set of characters, morphological or molecular, which is potentially available to the investigator at the time, without disregarding any subset of data. In recent phylogenetic studies on insects, for example, morphological characters from different semaphoronts, or several genetic loci, or a morphological and a molecular matrix have been combined and analyzed simultaneously in a 'supermatrix' (e.g. Lee et al. 2007; Miller et al. 2007; Winterton et al. 2007). Behavioral or ecological data are included less frequently, but progress is being made to make these data sources available and use the corresponding characters for phylogeny reconstruction (e.g. Wenzel 1992; Noll 2002; Freudenstein et al. 2003; Robillard et al. 2006).

Currently, many phylogenetic hypotheses are being based on molecular data only, even though in many instances morphological data are available (explicitly or implicitly). For example, Bybee et al. (2004) published a hypothetical phylogeny of Asilidae based on four genes

in 26 robber fly species. With the exception of a morphological phylogenetic study by Karl (1959), Bybee et al.'s (2004) hypothesis was the first truly phylogenetic reconstruction at a higher classificatory level, including most of the subfamily taxa recognized at the time (Dikow 2009). However, because only a few species were represented, the diversity of Asilidae could not be sampled adequately (Dikow 2009), and several of the conclusions were at odds with the classifications by Hull (1962) and Papavero (1973), which had been based on comparisons of morphological similarities. Bybee et al. (2004, p. 796) concluded that "many of the morphological characters used to define subfamilial groups … may be homoplastic," without actually testing the homology of morphological character states in a congruence test by including them in their data set. Dikow (2009) sampled 158 assassin-fly species and postulated the first extensive morphology-based hypothesis of evolutionary relationships within Asilidae, employing characters used by Hull (1962) and Papavero (1973) and adding many new character complexes. Some characters employed by Hull and Papavero in their classifications of Asilidae did not pass the congruence test (are not homologous at the secondary level). Other characters passed that test and have been shown to be homologous; these character states have been used in the subsequent phylogenetic classification (for details, see Dikow 2009). For about half of the species sampled by Dikow (2009), specimens for DNA extraction are available. Consequently, a total evidence analysis, adding molecular data to the morphological matrix, is presented here that includes all data currently available for Asilidae.

Phylogenetic analysis

The phylogenetic analysis was conducted in POY (Varón et al. 2008) by simultaneously aligning DNA sequences and searching for the most parsimonious trees, i.e. by direct optimization under dynamic homology (Wheeler 1996). This method was chosen because (1) it allows one to combine morphological characters (under static homology) and molecular characters (under dynamic homology) in a single matrix and analyze them simultaneously (see below); (2) the dynamic homology assessment is based strictly on parsimony as the optimality criterion, not on distance-based methods as in other alignment methods; and (3) hypotheses of homology of the so-called 'unalignable' regions of loops in ribosomal genes are based on the most parsimonious topology of relationships. By combining all data partitions (morphological and molecular ones), simultaneously aligning sequences and searching for trees in a single step, the structure that the morphological characters and the several genes

provide for the tree topology will affect the topographic homology assignment of nucleotide positions (alignment) of the other genes in a mutually informative way. For example, a taxon might be morphologically characterized by a number of autapomorphies, but the (more or less arbitrarily) chosen genetic loci, representing only a fraction of the entire genome, might lack such a specific signal. If one were to use the two-step approach of first aligning all genes separately, then in a second step conducting the tree search with the fixed alignments plus the morphological characters, one would disregard this reciprocal feedback of the data. On the other hand, the a priori primary homology assignment of the morphological character states can now be tested in light of the total evidence hypothesis and the most parsimonious topology derived from the entire data set in a simultaneous congruence test.

Choice of genetic loci

When early evolutionary diversification events are to be reconstructed with molecular data, the choice of gene loci is very important. The oldest fossils that can be unambiguously assigned to the Asilidae are Cretaceous in origin: from the Crato Formation, Brazil (Albian, approximately 110 million years ago; Grimaldi 1990) and from New Jersey amber, USA (Turonian, 94–90 million years ago; Grimaldi and Cumming 1999; Grimaldi and Engel 2005). Dikow (2009) showed that these two species belong to the crown group, and placed them well within the Asilidae. The two nuclear ribosomal genes 18S and 28S have been widely used in phylogenetic studies on Insecta and Diptera with similar diversification times. Among others, the two nuclear protein-encoding genes Elongation Factor-1 alpha (*EF-1α*; Friedlander et al. 1992) and the Carbamoylphosphate Synthase (CPS) domain of *CAD* (= rudimentary; Moulton and Wiegmann 2004, 2007) have been identified as suitable genetic markers for inferences on higher-level, Mesozoic divergences. Each of these four genes has been used in Diptera studies before (e.g. Wiegmann et al. 2000; Yang et al. 2000; Collins and Wiegmann 2002; Whiting 2002; Moulton 2003; Bybee et al. 2004; Moulton and Wiegmann 2004, 2007; Holston et al. 2007; Winterton et al. 2007). Danforth et al. (2005) summarized the application of these four genes among others in higher-level phylogenetic studies on insects in general, and concluded that they all provide information useful for the construction of evolutionary hypotheses on insects. Moulton (2003), in contrast, argued from a study of Simuliidae (Diptera) relationships that 28S and *EF-1α* are not particularly good molecular loci for Mesozoic divergences. Within the NSF-funded "Assembling the Tree of Life" Diptera project, which aims to elucidate the evolutionary history of the entire Diptera

based on a suite of molecular loci and morphological data (see http://www.inhs.uiuc.edu/cee/FLYTREE/), a number of novel gene loci for phylogenetic studies have been sequenced by Brian Wiegmann and coworkers in the molecular laboratory at North Carolina State University, Raleigh, NC, USA. One of these genes, the nuclear protein-encoding gene *AATS* (alanyl-tRNA synthetase), is included in the present analysis in addition to the four genes mentioned above.

Material and methods

Molecular protocols

Genomic DNA was extracted from either metathoracic leg or thoracic muscle tissue using the DNeasy tissue extraction kit (Quiagen, Valencia, CA, USA). AmpliTaq Ready-to-go PCR Beads (GE Healthcare, Buckinghamshire, UK) were used during polymerase chain reactions (PCR) and mixed with 2 μl DNA, 1 μl of 10 μM forward and reverse primer, and 21 μl H$_2$O. PCR was performed with standard protocols on a Mastercycler epgradient S (Eppendorf AG, Hamburg, Germany). The PCR products were cleaned with the AMPure magnetic bead system (Agencourt Bioscience Corporation, Beverly, MA, USA). Sequencing reactions were composed of 5 μl template, 1 μl Big Dye Terminator (version 1.1, Applied Biosystems, Foster City, CA, USA), 1 μl Big Dye Extender, and 1 μl of 3.2 μM primer, and amplified on the same PCR machines in 35 cycles of degeneration at 94 °C for 30 s, annealing at 50 °C for 1 min, and extension at 60 °C for 4 min. Products were cleaned with CleanSeq (Agencourt Bioscience Corporation, Beverly, MA, USA) before being sequenced on an ABI 3730xl DNA Analyzer. Sequences were edited in Sequencher (versions 4.5–4.8, Genes Code Corporation, Ann Arbor, MI, USA). Published primers for 18S, 28S, and *CAD* as well as unpublished primers from the Wiegmann laboratory for *AATS* and *EF-1α* are listed in Table 1. 28S rDNA was amplified in four fragments, 18S rDNA in three fragments, *CAD* in two fragments, and a single primer pair was used to obtain sequences of *AATS*. *EF-1α* sequences were obtained using four forward and three reverse primers. Initially, an approximately 1350 bp-long sequence of *EF-1α* was amplified in two fragments using the primer pairs 1F72/1R61 and 2F46/2R72L (Fig. 1). With these primers the success rate was limited, but it could be improved by using a newly designed primer (1F39) as a forward primer for the first fragment and a reverse primer designed by Danforth et al. (1999) for Halictidae (Hymenoptera) for the second fragment. The highest amplification success was obtained by using 1F39/1R61 and 2F46/2R53s or HaF2For/2R53s (Fig. 1), which amplifies approximately

Table 1. Primer sequences for genes amplified.

Gene fragment	Primer	Sequence	Source and remarks
18S 1	1F	TACCTGGTTGATCCTGCCAGTAG	Giribet et al. (1996)
	5R	CTTGGCAAATGCTTTCGC	Giribet et al. (1996)
18S 2	3F	GTTCGATTCCGGAGAGGGA	Giribet et al. (1996)
	Bi	GAGTCTCGTTCGTTATCGGA	Giribet et al. (1996)
18S 3	A2.0	ATGGTTGCAAAGCTGAAAC	Giribet et al. (1996)
	9R	GATCCTTCCGCAGGTTCACCTAC	Giribet et al. (1996)
28S 1	1a	CCCSCGTAAYTTAGGCATAT	Whiting (2002)
	4b	CCTTGGTCCGTGTTTCAAGAC	Whiting (2002)
28S 2	3.2a	AGTACGTGAAACCGTTCASGGGT	Whiting (2002)
	B	TCGGAAGGAACCAGCTACTA	Whiting (2002)
28S 3	4a	GGAGTCTAGCATGTGYGCAAGTC	Whiting (2002)
	5b	CCACAGCGCCAGTTCTGCTTACC	Whiting (2002)
28S 4	4.8a	ACCTATTCTCAAACTTTAAATGG	Whiting (2002)
	7b1	GACTTCCCTTACCTACAT	Whiting (2002)
AATS	1F40	GNATGAAYCARTTYAARCCNAT	J. Kim and B. Wiegmann pers. comm.
	1R244	CATNCCRCARTCNATRTGYTT	J. Kim and B. Wiegmann pers. comm.
CAD 4	4F787	GGDGTNACNACNGCNTGYTTYGARCC	Moulton and Wiegmann (2004)
	4R1098	TTNGGNAGYTGNCCNCCCAT	Moulton and Wiegmann (2004)
CAD 5	5F1057	ACNGAYTAYGAYATGTGYGA	Wiegmann et al. unpublished
	5R1278	TCRTTNTTYTTWGCRATYAAYTGCAT	Moulton and Wiegmann (2004)
EF-1α 1	1F72	GGGCAAGGAAAAGATTCACATTAAC	S. Scheffer and B. Wiegmann pers. comm. (= EF72F)
	1F39	CACCACTGGACATTTGATTTA	designed for present study
	1R61	GATGGTTCCAACATGTTGTC	S. Scheffer and B. Wiegmann pers. comm. (= AGEF61R)
EF-1α 2	2F46	TGAGGAAATCAAGAAGGAAG	S. Scheffer and B. Wiegmann pers. comm. (= EF46F)
	HaF2For	GGGYAAAGGWTCCTTCAARTATGC	Danforth et al. (1999)
	2R53S	GCGAACTTGCAAGCAATGTGAGC	S. Scheffer and B. Wiegmann pers. comm. (= EF53R)
	2R71L	CTTGCCCTTGGTGGCCTTCTCGG	S. Scheffer and B. Wiegmann pers. comm. (= EF71R)
	M13F	TGTAAAACGACGGCCAGT	
	M13R	CAGGAAACAGCTATGAC	

1100 bp of the gene, and is part of the longer sequence obtained by using 1F72/1R61 and 2F46/2R72L. To increase the amplification success, particularly among the nuclear protein-encoding genes, primers tagged with an M13 tail were used in many instances. M13 primers alone were used as the sequencing primers when tailed primers were used for the initial amplification, whereas in all other instances the amplification primers were used as the sequencing primers. Overall, some 7300 bp of DNA sequence are included in the present analysis: 2000 bp of 18S, 2200 bp of 28S, 550 bp of *AATS*, 1405 bp of *CAD*, and 1100 bp of *EF-1α*. GenBank accession and voucher specimen numbers are provided in Table 2, while the systematic positions of species, the geographic origin of specimens, and the completeness of the included gene fragments are summarized in Appendix 1 in the online version of this paper.

Taxon sampling

Obtaining comprehensive, combined morphological and DNA sequence data sets is not always possible due to lack of taxon overlap (e.g. Nixon and Carpenter 1996; Malia et al. 2003). Nixon and Carpenter (1996) suggested several methods to combine data matrices when the terminal taxa are not coinciding. Many species included in the morphological phylogeny by Dikow (2009) are rarely collected and have not yet been preserved properly for DNA extraction and sequencing.
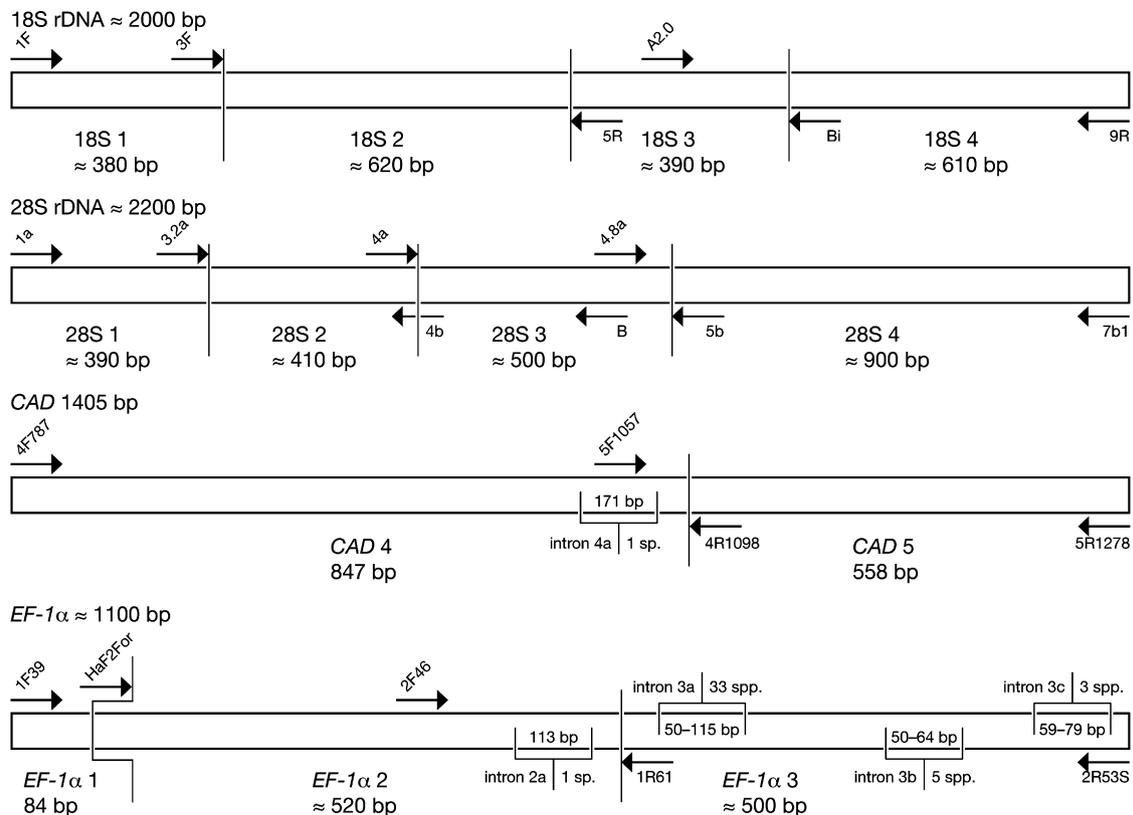
Fig. 1. Schematic maps of genes, with amplification primers and cutting points for fragments for POY analysis indicated. In *CAD* and *EF-1α*, positions and lengths of spliceosomal introns shown, as well as numbers of species exhibiting the latter.

Of the 158 Asilidae species represented in Dikow (2009), 77 have been preserved in 96% ethanol and are included in the present analysis (Table 2, Appendix 1). In this sampling, 12 of the 14 subfamily taxa proposed by Dikow (2009) are represented with multiple exemplars; only the two species-poor southern hemisphere taxa Bathypogoninae and Phellinae, as well as the genera incertae sedis, *Coleomyia* Wilcox & Martin, 1935 and *Oligopogon* Loew, 1847, are unrepresented. However, all previously recognized subfamily taxa (Papavero 1973; Geller-Grimm 2004) are represented by multiple exemplars (Appendix 1). The outgroup taxa are also sampled extensively; 11 of the 15 species used by Dikow (2009) are incorporated here (Table 2, Appendix 1). Nemestrinidae is not represented in the present analysis, as no specimens were available; Bombyliidae is only represented by *Bombylius major* Linnaeus, 1758. This species is always used as the root of the cladograms, as it has been shown to be the species least closely related to Asilidae within Asiloidea in the morphological phylogeny by Dikow (2009) and also in previous hypotheses of Asiloidea relationships (e.g. Hennig 1973; Woodley 1989; Yeates 1994; Yeates and Irwin 1996). In contrast, both Yeates (2002) and Bybee et al. (2004) postulated Asilidae to be the sister-taxon to the remaining Asiloidea except Bombyliidae. In seven cases for which

the species identification is not certain, thus is given as 'sp.' below, it has been verified that all respective specimens belong to a single species. An additional term in parentheses denoting the collecting locality is added to those provisional names as a reference for future studies. These species are either undescribed, or belong to speciose genera which need to be revised before species identifications can be undertaken.

Phylogenetic analysis

The present phylogenetic study is based on parsimony as the optimality criterion to allow every character state (A, C, G, T, gap, and all states in the morphological matrix) to evolve independently of each other in every part of the tree and at any position on a branch. In addition, all character transformations were equally weighted, i.e. non-additive coding was used for morphological characters and the same cost for transitions, transversions, and gaps in molecular data. POY (Phylogenetic Analysis of DNA and other Data using Dynamic Homology, version 4.0.2870; Varón et al. 2008) was used for simultaneous alignment and parsimony tree searches of the combined data set composed of morphological and molecular data as well as of the

Table 2. Voucher specimen identifiers ("Asil", "OUT": in author's collection; "NMSA": to be deposited at Natal Museum, Pietermaritzburg, South Africa) and GenBank accession numbers for DNA sequences generated in present study.

Species	Voucher	18S	28S	*AATS*	*CAD*	*EF-1α*
Leptogaster cylindrica	Asil-1	EF650101	EF650188	EF650299	EF650339	EF650414
Lasiopogon cinctus	Asil-2	EF650102	EF650189	EF650314	EF650341	EF650415
Dasypogon diadema	Asil-4	EF650103	EF650190	EF650281	EF650342	EF650416
Dioctria atricapillus	Asil-7	EF650159	EF650191	EF650287	EF650406	EF650417
Leptarthrus brevirostris	Asil-8	EF650104	EF650192		EF650343	EF650418
Dasophrys crenulatus	Asil-17	EF650105	EF650193		EF650344	EF650419
Perasis transvaalensis	Asil-24	EF650106	EF650194			EF650420
Neolophonotus bimaculatus	Asil-36	EF650107	EF650195	EF650271	EF650345	EF650421
Euscelidia pulchra	Asil-39	EF650108	EF650196		EF650346	EF650422
Lasiocnemus lugens	Asil-40	EF650109	EF650197	EF650297		EF650423
Choerades bella	Asil-41	EF650110	EF650198	EF650290	EF650348	EF650424
Microstylum sp. (Karkloof)	Asil-43	EF650166	EF650199		EF650349	EF650477
Pegesimallus laticornis	Asil-44	EF650111	EF650200	EF650285	EF650350	EF650425
Gonioscelis ventralis	Asil-45	EF650112	EF650201	EF650305	EF650351	EF650426
Trichardis effrena	Asil-53	EF650113	EF650202	EF650296	EF650352	EF650427
Stiphrolamyra angularis	Asil-56	EF650114	EF650203		EF650353	EF650428
Acnephalum cylindricum	Asil-57	EF650115	EF650204	EF650303	EF650355	EF650429
Lycostommyia albifacies	Asil-66	EF650116	EF650205	EF650306	EF650356	EF650430
Trichoura sp. (Tierberg)	Asil-67	EF650172	EF650206		EF650354	
Hoplistomerus nobilis	Asil-70	EF650117	EF650207		EF650357	EF650431
Laxenecera albicincta	Asil-71	EF650118	EF650208	EF650292	EF650358	EF650432
Rhipidocephala sp. (Harold Johnson)	Asil-72	EF650119	EF650209		EF650359	EF650433
Afroestricus chiastoneurus	Asil-77	EF650120	EF650210	EF650301	EF650360	EF650434
Stichopogon punctum	Asil-80	EF650121	EF650211	EF650315	EF650361	EF650435
Promachus amastrus	Asil-82	EF650122	EF650212		EF650363	EF650436
Philodicus tenuipes	Asil-83	EF650152	EF650213	EF650272	EF650364	EF650437
Dysmachus trigonus	Asil-88	EF650156	EF650214	EF650277	EF650366	EF650438
Tolmerus atricapillus	Asil-89	EF650123	EF650215	EF650280	EF650367	EF650439
Philonicus albiceps	Asil-90	EF650124	EF650216	EF650279	EF650368	EF650440
Neoitamus cyanurus	Asil-91	EF650176	EF650263	EF650327	EF650405	EF650479
Dioctria rufipes	Asil-92	EF650125	EF650217			EF650441
Beameromyia bifida	Asil-97	EF650126	EF650218		EF650365	EF650442
Tipulogaster glabrata	Asil-98	EF650127	EF650219			EF650443
Connomyia varipennis	Asil-103	EF650128	EF650220	EF650304	EF650369	EF650444
Scylaticus costalis	Asil-110	EF650170	EF650221	EF650310		EF650445
Laphria aktis	Asil-114	EF650129	EF650222		EF650372	EF650446
Holcocephala calva	Asil-115	EF650130	EF650223	EF650319	EF650373	
Holcocephala abdominalis	Asil-116	EF650131	EF650224		EF650374	
Proctacanthus philadelphicus	Asil-117	EF650154	EF650225	EF650274	EF650375	EF650447
Lestomyia fraudiger	Asil-125	EF650132	EF650226	EF650283	EF650376	EF650448
Saropogon luteus	Asil-130	EF650133	EF650227	EF650286	EF650377	EF650449
Eudioctria albius	Asil-133	EF650134	EF650228			EF650450
Leptogaster arida	Asil-136	EF650135	EF650229	EF650298	EF650362	EF650451
Pogonioefferia pogonias	Asil-140	EF650153	EF650230	EF650273	EF650378	EF650452
Pilica formidolosa	Asil-144	EF650163	EF650231	EF650294	EF650379	
Cerotainia albipilosa	Asil-151	EF650160	EF650232	EF650289	EF650380	
Tillobroma punctipennis	Asil-167	EF650171	EF650233	EF650311		
Molobratia teutonus	Asil-170	EF650136	EF650234	EF650284	EF650382	EF650453
Asilus crabroniformis	Asil-171	EF650137	EF650235	EF650275	EF650383	EF650454
Asilus sericeus	Asil-172	EF650138	EF650236	EF650276	EF650384	EF650455
Megaphorus pulchrus	Asil-173	EF650151	EF650237		EF650385	
Emphysomera conopsoides	Asil-182	EF650164	EF650238		EF650386	EF650456
Emphysomera pallidapex	Asil-202	EF650139	EF650239	EF650300	EF650387	EF650457
Stichopogon elegantulus	Asil-233	EF650140	EF650240		EF650388	EF650458
Stenopogon rufibarbis	Asil-236	EF650141	EF650241			EF650459
Ablautus coquilletti	Asil-249	EF650142	EF650242			EF650460

Table 2. (*continued*)

Species	Voucher	18S	28S	*AATS*	*CAD*	*EF-1α*
Prolepsis tristis	Asil-255	EF650168	EF650243	EF650308	EF650389	EF650478
Dioctria hyalipennis	Asil-263	EF650143	EF650244		EF650390	EF650461
Laphystia tolandi	Asil-274	EF650144	EF650245	EF650295	EF650371	EF650462
Diogmites grossus	Asil-277	EF650145	EF650246	EF650282	EF650391	EF650475
Cyrtopogon rattus	Asil-278	EF650146	EF650247		EF650392	EF650463
Lasiopogon aldrichii	Asil-287	EF650174	EF650248	EF650313	EF650393	EF650464
Clephydroneura sp. (Kepong)	Asil-289	EF650155	EF650249		EF650394	EF650465
Machimus occidentalis	Asil-296	EF650157	EF650250	EF650278	EF650395	EF650466
Plesiomma sp. (Guanacaste)	Asil-302	EF650167	EF650251	EF650307	EF650340	EF650467
Ceraturgus fasciatus	Asil-303	EF650165	EF650252		EF650396	EF650468
Ommatius tibialis	Asil-305	EF650147	EF650253	EF650302	EF650397	EF650469
Atomosia puella	Asil-321	EF650148	EF650254	EF650288	EF650398	
Nicocles politus	Asil-330	EF650158	EF650255			EF650470
Stichopogon trifasciatus	Asil-331	EF650175	EF650256	EF650316	EF650399	EF650471
Willistonina bilineata	Asil-334	EF650173	EF650257	EF650312	EF650400	EF650472
Ospriocerus aeacus	Asil-370	EU410377	EU410378	EU410379	EU410380	EU410381
Lamyra gulo	NMSA-1	EF650161	EF650258	EF650291	EF650401	EF650476
Nusa infumata	NMSA-2	EF650162	EF650259	EF650293	EF650402	
Damalis monochaetes	NMSA-12	EF650149	EF650260	EF650318	EF650403	EF650473
Damalis annulata	NMSA-76	EF650150	EF650261	EF650317	EF650404	
Rhabdogaster pedion	NMSA-83	EF650169	EF650262	EF650309		EF650474
Phycus frommeri	OUT-1	EF650091	EF650178	EF650265	EF650329	EF650407
Apsilocephala longistyla	OUT-2	EF650092	EF650179		EF650330	
Prorates sp. (Escalante)	OUT-4	EF650093	EF650180		EF650332	EF650408
Opomydas townsendi	OUT-6	EF650094	EF650181	EF650268	EF650333	EF650409
Nemomydas brachyrhynchus	OUT-7	EF650095	EF650182		EF650334	
Apiocera painteri	OUT-8	EF650096	EF650183		EF650335	EF650411
Hemigephyra atra	OUT-9	EF650097	EF650184	EF650266	EF650331	EF650410
Afroleptomydas sp. (Clanwilliam)	OUT-11	EF650098	EF650185	EF650270	EF650336	
Bombylius major	OUT-12	EF650090	EF650177	EF650264	EF650328	
Mitrodetus dentitarsis	OUT-18	EF650099	EF650186	EF650267	EF650337	EF650412
Mydas clavatus	OUT-25	EF650100	EF650187	EF650269	EF650338	EF650413

molecular-only data set. Initially, POY was available only as a Beta version and the tree searches were done in several versions, including builds 1915, 2635, and 2850, but all results were later checked with the released version 4.0.2870. POY was run on two computers at various stages of this project: (1) on a Penguin Computing cluster computer (San Francisco, CA, USA; 33 nodes, including master, with two dual-core 3.0 GHz Intel XEON 5160 CPUs, 16 GB RAM, Infiniband interconnect) at the Computational Sciences facility at the American Museum of Natural History, New York, NY, USA, and (2) on an Apple MacPro desktop (2 × 2.66 GHz Dual-Core Intel Xeon, 6 GB RAM). The parsimony ratchet (Nixon 1999) and tree fusing (Goloboff 1999) were used in addition to regular branch swapping algorithms to find the most parsimonious topology. The tree search was divided into four main searches: (1) building 100 Wagner trees and swapping each, (2) submitting the resulting trees to the ratchet, (3) submitting these trees to tree fusing, and (4) selecting the best tree(s) and rediagnosing it (them)

under iterative pass optimization (Wheeler 2003) followed by exhaustive swapping. The following provides the commands used to search for most-parsimonious trees in POY (semicolons indicate positions of hard returns in search script):

set(log:new:"file.log"); read("file1.seq","file2.seq",.., "file3.ss"); set(root:"Bombylius_major"); transform ((all,tcm:(1,1))); build(trees:100); swap(); report("file_ buildtrees.tre",trees); perturb(transform((all,static_approx)), ratchet:(0.25,3), iterations:20); fuse(swap()); select(); set(iterative); swap(around); report("filetree.ps",graph-trees,"filetree.tre",trees); quit().

Explanation of commands: open log file; read sequence files and morphological matrix; set *Bombylius major* as the default outgroup; weight all data equally and set transition-transversion cost as well as gap cost to 1; build 100 Wagner trees; swap each of the 100 Wagner trees; report all Wagner trees in a file; perform 20 iterations of the ratchet on every tree by weighting 25% of the nucleotide columns by a factor of 3 (note: this is the original implementation of the ratchet by

Nixon 1999 and not the default in POY, which would only weight gene partitions differently); perform the default number of iterations of tree fusing on the loaded trees; select the optimal tree; set the optimization algorithm to iterative pass and rediagnose tree(s); swap the tree(s) by completely exploring the neighborhood and choosing the best swap position before continuing; report a Postscript and a POY treefile; quit POY.

The implied alignment was obtained with "report ("file.ia",ia:names:("file.seq"))" after reading all data files, setting the default outgroup, reading the shortest tree, transforming all data, and changing to iterative pass optimization. Bremer support (Bremer 1988, 1994) was used to assess branch support and computed in POY. The search for suboptimal trees was implemented by saving all visited trees during the search for the most parsimonious cladogram in a separate file (command "visited:"file.tre"" within the swap command). The following commands evaluated all saved trees and calculated Bremer support values in reference to the most parsimonious topology: read("file1.seq", "file2. seq",...,"file3.ss","mptree.tre"); set(root:"Bombylius_ major"); transform((all,tcm:(1,1))); set(iterative); report ("file.ps",graphsupports:bremer:"alltrees.tre"). More than 390 million suboptimal topologies were stored and evaluated for the total evidence hypothesis.

When this project was nearly finished, POY version 4.0.2870 was released and a new 'search' command was implemented. This command allows the user to specify a maximum time and RAM allowance for tree searches. The search algorithm will now fit as many exhaustive tree searches as possible in the specified time and attempt to stay within the limits of RAM available. This very powerful implementation was used as well at the end of this project and found the most parsimonious tree within 24 h of running on the desktop computer, which is much faster than with the manual tree searches outlined above.

WinClada (version 1.00.08; Nixon 2002) was used to evaluate the character optimization with the following nomenclature applied: unambiguous, slow (= DELTRAN of MacClade), and fast (= ACCTRAN of MacClade). The morphology-only analysis was conducted in TNT (Tree search using New Technologies, version 1.1 of December 2007; Goloboff et al. 2008) under UNIX on the Apple MacPro desktop computer. Both the tree search and the Bremer support/relative Bremer support (Goloboff and Farris 2001) calculations implemented the same strategy as in Dikow (2009).

Preparation of sequence data set

Direct optimization (Wheeler 1996) and iterative pass optimization (Wheeler 2003) as implemented in POY are computationally very time consuming. Reducing the length of each sequence by slicing the genes into shorter fragments/partitions decreases computation time, because fewer nucleotides need to be optimized at internal nodes (Giribet 2001). With the exception of AATS, which is only 550 bp long, all genes were cut into several gene fragments. Primer sites were used to cut the sequences at homologous sites as illustrated in Fig. 1. These sequence fragments (four for both 18S and 28S, three for EF-1α, and two for CAD) were then concatenated in the text editor TextWrangler and delimited by a pound symbol (#), indicating to POY the end of a gene fragment. By aligning every fragment separately in SeaView (version 2.2; Galtier et al. 1996) and Muscle (version 3.6; Edgar 2004), as well as by inspecting the implied alignment of an initial search in POY prior to the phylogenetic analysis, it was verified that the slicing was done correctly and no nucleotides were placed wrongly in an adjacent fragment. Slicing the genes in fragments allows the inclusion of incomplete sequences for species for which a particular fragment is missing (see Appendix 1), and allows the inclusion of introns, which were also delimited by pound symbols based on an initial analysis (see Fig. 1 and the Results section below). The delimited sequence data files are available from the supplementary material in the online edition of this paper, as well as from: http://www. tdvia.de/research/research_data.html.

Morphological data set

The morphological matrix for the total evidence analysis was adopted from Dikow (2009), which includes a detailed description of characters and character states. As only 77 of the 158 Asilidae species are represented with molecular data in the present analysis, nine morphological characters became uninformative. These are: (1) character #16, medial projection on postgenae – autapomorphy of Apioceridae and uninformative because only a single species of Apioceridae is included; (2) #17, shape of proboscis – uninformative because all species except Pilica formidolosa possess a straight proboscis; (3) #50, elevated ridge medially on frons – uninformative as developed only in Cerotainia albipilosa; (4) #84, katatergite shape – uninformative as all taxa included possess a more or less flat sclerite; (5–6) #87, stout and erect macrosetae on anterior mesonotum, and #117, cuticular facets medially on proximal metathoracic femora – species representing these character states not represented in present analysis; (7) #139, presence of discal medial cell – uninformative as found only in Bombyliidae, of which only a single species was included here; (8) #157, sclerotization of abdominal tergites 3–6 – uninformative as Rhipidocephala sp. (Harold Johnson) is the only species exhibiting unsclerotized tergites; (9) #194, shape

of abdominal sternite 8 in males – all species either possess a simple rectangular sclerite or the character is not applicable. The morphological matrix therefore consists of 211 parsimony informative characters; it can be downloaded from the TreeBase web-site (study accession number: S2293; matrix accession number: M4353) as well from: http://www.tdvia.de/research/research_data.html. To minimize confusion, all character numbers mentioned in the Results section correspond to those in Dikow (2009).

The terms adelphotaxon, sister group, and sister taxon are used interchangeably. Autapomorphy is used for a non-homoplasious acquisition of a state (globally uncontradicted and unreversed apomorphic character state), for which the transformation from plesiomorphic to apomorphic is optimized at the root of a particular taxon (one to many species) and therefore postulated to be part of its ground pattern. An apomorphic character state has been acquired independently more than once, is autapomorphic locally, but is found somewhere else in the tree either through convergence or reversal and therefore is homoplasious. The names of all included species are listed with taxonomic authorship and publication year in Appendix 1; this information is omitted below.

Results

Total evidence analysis

The parsimony analysis of the combined data set in POY resulted in a single most parsimonious tree (Fig. 2) of cost 27,582 (iterative pass optimization, CI = 0.20 and RI = 0.49 with uninformative characters excluded; 27,703 under direct optimization). The implied alignment for this topology can be downloaded as a whole from the TreeBase website (study accession number: S2293; matrix accession number: M4354) and as a whole as well as separately for each gene from: http://www.tdvia.de/research/research_data.html.

Asilidae is supported as monophyletic, with the sister taxon composed of Apioceridae plus Mydidae (Figs. 2, 3; Table 3). Six of the included 12 subfamily taxa of robber flies are recovered as monophyletic, whereas the remaining 6 are non-monophyletic (Table 3).

Asilidae is corroborated as monophyletic with the following morphological autapomorphies that are unambiguously optimized at its root (Fig. 3): hypopharynx heavily sclerotized (character 30: state 1), hypopharynx with dorsal seta-like spicules (33: 1), labrum short, at most half as long as labium (34: 1), dorso-posterior margin of cibarium with one transverse ridge connecting cornua (35: 1), cibarium trapezoidal (36: 0), cibarium with median longitudinal ridge (38: 1), and prothoracic

tibiae with at least three setae antero-ventrally (105: 1). Additional unambiguously optimized apomorphic character states, which are either also present in some outgroup taxa or not in all robber flies, are: apex of labella pointed (24: 1), at least some median ommatidia in compound eye larger than lateral ones (46: 1), postpronotal lobes extending medially (72: 1), and katatergal setae represented by macrosetae and regular setae (83: 2).

Under fast optimization, no additional autapomorphy is optimized at the root of Asilidae, and the following are additional apomorphies: cross-section of prementum proximally circular (18: 0), labella reduced and fused to prementum only ventrally (23: 1), hypopharynx as long as labium (31: 1), anterior anepisternal setae erect (78: 1), prothoracic and mesothoracic coxae more or less directed ventrally (109: 1), wing cell m_3 open (135: 0), spurs on female ovipositor absent (174: 0), male epandrium and hypandrium approximating proximally but not fused (201: 1), and male sperm sac appearing weakly sclerotized (218: 0).

Under slow optimization, no additional autapomorphy is optimized at the root of Asilidae, and the following are additional apomorphies: vertex slightly depressed between compound eyes (3: 1), mystax (facial setae) present (6: 1), stipites of maxilla fused medially (15: 1), hypopharynx as long as labium (31: 1), hypopharynx parallel-sided throughout, only distal tip suddenly pointed (32: 0), anterior anepisternal setae erect (78: 1), and proximal prothoracic tarsomere shorter than or as long as following two tarsomeres combined (120: 0).

Evaluating the DNA sequence data, 25 autapomorphies (18S = 7, 28S = 3, $AATS$ = 3, CAD = 6, EF-1α = 6) and 25 apomorphies (18S = 3, 28S = 1, $AATS$ = 3, CAD = 14, EF-1α = 4) are unambiguously optimized at the root of Asilidae (Fig. 3, Table 4).

Among the DNA data, CAD provides a large number of autapomorphies and apomorphies supporting certain clades – in contrast to EF-1α, which provides relatively few such characters (Table 4). It has to be kept in mind, though, that EF-1α has been sequenced for relatively fewer taxa than 18S, for example, which is complete for all but two species (Appendix 1). During sequence alignment and tree search, gaps were inserted to obtain hypotheses of topographic homology of nucleotides, resulting in increased lengths of the five loci in the implied alignment: 18S extended from ≈ 2000 to 2488 bp, 28S from ≈ 2200 to 4151 bp, $AATS$ from 550 to 562 bp, CAD from 1405 to 1446 bp without intron (1617 bp with intron; Fig. 1), and EF-1α from ≈ 1000 to 1027 bp without introns (1555 bp with introns; Fig. 1). The overall length of the implied alignment is 9675 bp without introns, of which 2290 bp are parsimony informative and 7385 bp are parsimony uninformative (10,373 bp with introns, 2367 bp informative, 8006 bp uninformative).
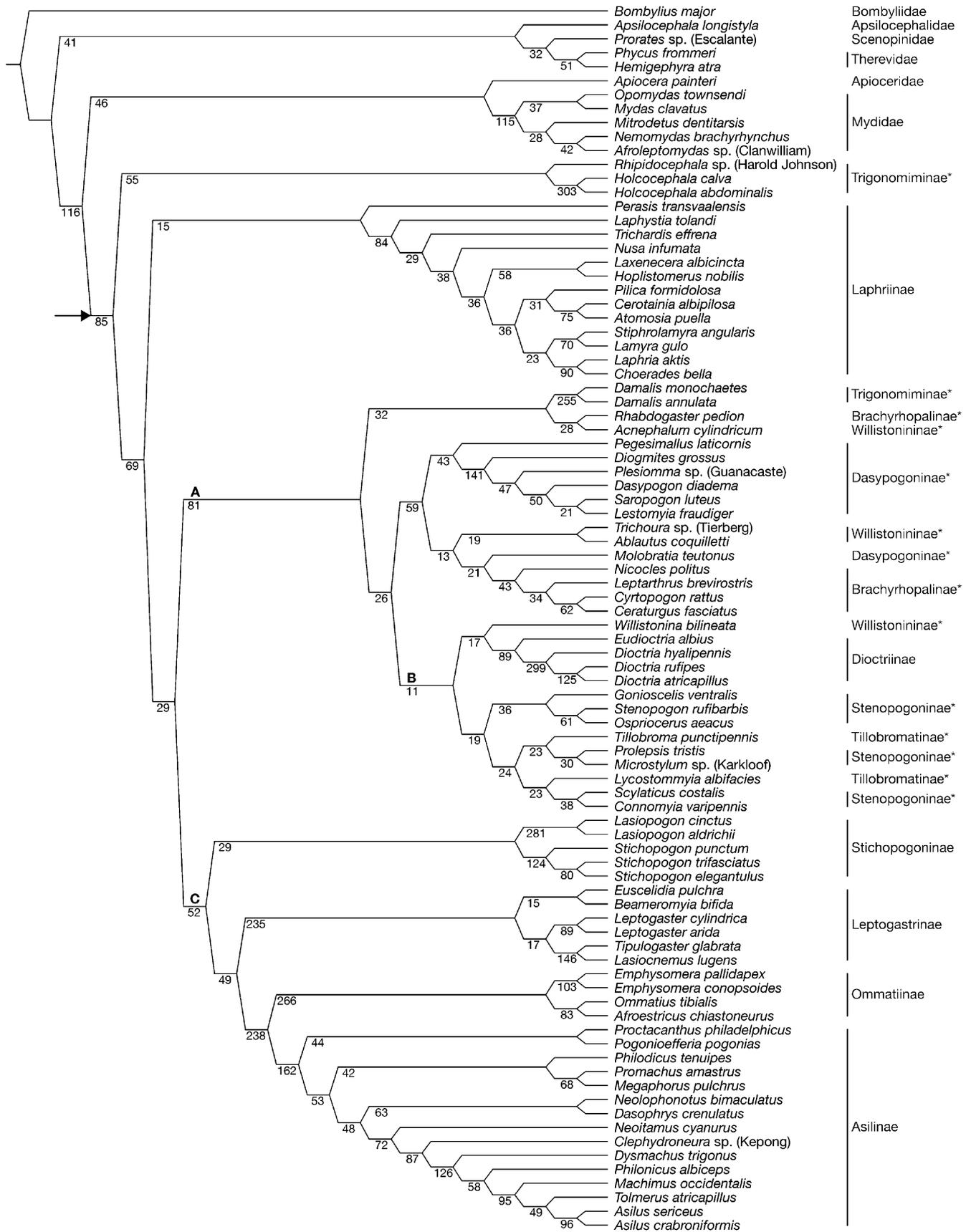
Fig. 2. Most parsimonious cladogram (27,582 steps; CI = 0.20; RI = 0.49) from combined analysis of equally weighted morphological and DNA sequence data in POY. Bremer support values below branches. Letters A to C label clades referred to in the text and Table 4. Arrow indicates root of Asilidae. Asterisks (*) mark non-monophyletic subfamily taxa.

Fig. 3. Total evidence cladogram as in Fig. 2, with character optimization and distribution mapped onto it (unambiguous optimization). Solid circles on branches represent morphological autapomorphies, with respective character number shown above and character state below. Solid squares indicate molecular autapomorphies. Letters A to C label clades referred to in the text and Table 4. Arrow indicates root of Asilidae.

The optimization of morphological character states and number of autapomorphic molecular changes unambiguously optimized at the root of the respective monophyletic subfamily taxon is as follows (Table 4).

Table 3. Monophyly evaluation for subfamily taxa in Asilidae (see Dikow 2009) and for sister group of Asilidae (Api = Apioceridae; Myd = Mydidae) based on total-evidence, morphology-only, and molecular-only analysis, respectively.

Taxon	Total (Figs. 2, 3)	Morphology (Fig. 4)	Molecular (Fig. 5)
Asilinae	•	•	•
Bathypogoninae	/	/	/
Brachyrhopalinae	–	–	–
Dasypogoninae	–	–	–
Dioctriinae	•	•	•
Laphriinae	•	•	–
Leptogastrinae	•	•	•
Ommatiinae	•	•	•
Phellinae	/	/	/
Stenopogoninae	–	–	–
Stichopogoninae	•	•	–
Tillobromatinae	–	–	–
Trigonomiminae	–	•	–
Willistonininae	–	–	–
Api + Myd	Api + Myd	Api	Api + Myd

Symbols: • = monophyletic; – = non-monophyletic; / = no representative analyzed.

Laphriinae. Autapomorphies: dorsal margin of postocciput with triangular projection (42: 1), male abdominal tergites 7–8 and sternite 7 reduced while sternite 8 is well-developed (193: 3); no molecular autapomorphies. Additional apomorphies: 14: 1; 57: 1; 85: 1; 100: 1; 131: 2; 144: 1; 172: 5; 197: 0; 206: 1; 215: 1.

Dioctriinae. Autapomorphies: no morphological autapomorphies; $18S = 2$, $28S = 3$, $EF-1\alpha = 2$. Additional apomorphies: 3: 2; 12: 0; 22: 0; 53: 1; 62: 1; 79: 2; 91: 0; 118: 2; 154: 1; 168: 0; 169: 0; 172: 0; 173: 2; 174: 0; 184: 1; 193: 4; 201: 0; 211: 1.

Stichopogoninae. Autapomorphies: posterior compound eye margin distinctly sinuate in ventral half (64: 2); $18S = 1$, $28S = 3$, $EF-1\alpha = 1$. Additional apomorphies: 14: 2; 28: 1; 48: 1; 122: 0; 143: 1; 170: 6; 185: 2.

Leptogastrinae. Autapomorphies: lateral postpronotal setae absent (70: 0), postpronotal lobes extending medially and anteriorly, nearly touching medially (72: 2), metathoracic coxa directed anteriorly (111: 1), abdominal tergite 2 more than twice as long as wide (153: 2), abdominal sternite 2 divided medially into two equal halves separated by fenestra (159: 1), male with surstylus on epandrium (198: 1), male with lateral processes of gonostyli (207: 1); $18S = 3$, $28S = 8$, $CAD = 5$, $EF-1\alpha = 1$. Additional apomorphies: 23: 2; 33: 2; 78: 2; 79: 2; 83: 1; 91: 0; 102: 1; 104: 0; 110: 0; 123: 0; 125: 1; 178: 0; 203: 1; 204: 0.

Table 4. Numbers of unambiguously optimized autapomorphic and apomorphic character changes for all data partitions and selected clades in the total evidence hypothesis (Figs. 2, 3).

Taxon	18S		28S		AATS		CAD		EF–1α		Morphology	
	aut	apo	aut	apo	aut	apo	aut	apo	aut	apo	aut	apo
Asilidae	7	3	3	1	3	3	6	14	6	4	7	4
Holcocephala + Rhipidocephala	1	8	7	17	–	–	–	24	–	–	–	8
Holcocephala	8	24	6	31	–	–	2	39	–	–	1	11
Rhipidocephala	3	15	23	28	–	–	3	71	–	–	2	6
Laphriinae	–	2	–	8	–	–	–	–	–	4	2	10
Clade A	–	1	–	2	–	3	–	13	–	1	–	4
(*Damalis* (*Acnephalum Rhabdogaster*))	–	1	–	7	–	15	3	25	–	2	–	4
Damalis	14	34	6	37	1	21	4	87	–	–	2	18
Acnephalum + Rhabdogaster	–	3	–	–	1	9	–	–	–	7	–	3
Clade B	–	–	–	1	–	6	–	8	–	6	–	1
Dioctriinae	2	12	3	30	–	–	–	–	2	12	–	18
Clade C	–	2	4	2	1	16	–	23	–	6	–	3
Stichopogoninae	1	6	3	8	–	7	–	17	1	7	1	7
(Leptogastrinae (Asilinae Ommatiinae))	–	3	2	12	1	8	–	23	–	12	–	4
Leptogastrinae	3	13	8	34	–	–	5	73	1	25	7	17
Asilinae + Ommatiinae	3	8	3	16	1	7	–	29	–	12	1	13
Ommatiinae	14	23	8	29	2	13	–	38	–	14	2	6
Asilinae	–	1	1	7	1	9	–	22	–	2	1	3
(Asilidae (Apioceridae Mydidae))	–	2	5	7	1	6	4	10	–	–	1	5
Apioceridae + Mydidae	1	3	–	5	–	–	–	21	–	7	3	4
Mydidae	3	4	1	10	–	–	1	15	–	10	15	18

Ommatiinae. Autapomorphies: setae on antennal stylus on anterior surface (59: 1), female with marginal macrosetae on abdominal tergite 7 (165: 1); 18S = 14, 28S = 8, *AATS* = 2. Additional apomorphies: 14: 1; 102: 3; 153: 1; 162: 1; 163: 1; 164: 1.

Asilinae. Autapomorphies: male with gonostyli positioned distally on gonocoxites (206: 0); 28S = 1, *AATS* = 1. Additional apomorphies: 55: 1; 64: 1; 170: 2/3.

The clade Asilidae + (Apioceridae + Mydidae) is supported by a single unambiguously optimized morphological autapomorphy, i.e. lateral depression on prothoracic coxa present (104: 1), as well as by the following numbers of molecular autapomorphies: 28S = 5, *AATS* = 1, and *CAD* = 4. Additional unambiguously optimized morphological apomorphies are: 12: 0; 68: 1; 76: 1; 180: 0; 197: 1. Under fast optimization, the following autapomorphies can be added: mystax (facial setae) present (6: 1), stipites of labium fused to postgenae (15: 1), female abdominal tergite 9 small and triangular (171: 0).

The monophyly of the clade Apioceridae plus Mydidae is supported by three autapomorphies, i.e. anterior ocellus separated from posterior ocelli (60: 1), pulvilli with a single dorsal ridge (124: 0), wing vein M_1 terminating anterior to wing apex (147: 0), by a single autapomorphic change in 18S, and by the following additional apomorphic character states: 79: 0; 127: 2; 131: 1; 169: 1.

The monophyly of Apioceridae could not be tested, but the monophyly of Mydidae is supported by 15 morphological autapomorphies, i.e. 5: 2; 9: 0; 43: 1; 52: 0; 56: 1; 61: 1; 76: 2; 77: 1; 89: 0; 132: 1; 143: 3; 148: 1; 155: 1; 192: 1; 205: 0, as well as by 3 autapomorphies in 18S, 1 in 28S, 1 in *CAD*, and by several apomorphies: 4: 4; 11: 0; 27: 0; 28: 2; 39: 0; 44: 2; 57: 4; 58: 3; 63: 1; 71: 1; 86: 1; 97: 0; 98: 0; 100: 1; 101: 1; 202: 2; 213: 0; 215: 1.

Morphology-only analyses

The equally weighted parsimony analysis of the morphological matrix in TNT resulted in 18 most parsimonious trees of length 1606 (CI = 0.22, RI = 0.66); the strict consensus topology has 1625 steps (Fig. 4; CI = 0.21, RI = 0.65, 8 nodes collapsed). Asilidae is supported as monophyletic and 7 of the 12 subfamily taxa are recovered as monophyletic (Table 3).

The following characters are unambiguously optimized as autapomorphies at the root of Asilidae: 30: 1; 33: 1; 34: 1; 36: 1; 109: 1; apomorphic character changes are: 3: 2; 4: 2; 6: 1; 18: 0; 23: 2; 31: 1; 46: 1; 72: 1; 78: 1; 83: 2; 105: 1; 113: 0; 120: 0; 121: 0.

The respective unambiguously optimized autapomorphies and apomorphic character changes for monophyletic subfamily taxa are as follows.

Leptogastrinae. Autapomorphies: 70: 0; 72: 2; 111: 1; 137: 1; 153: 2; 159: 1; 198: 1; 207: 1; apomorphies: 4: 1; 12: 1; 33: 2; 69: 0; 78: 2; 79: 2; 96: 2; 98: 1; 104: 0; 110: 0; 122: 0; 123: 0; 125: 1; 130: 2; 135: 0; 143: 2; 177: 1; 178: 0; 203: 1; 204: 0.

Ommatiinae. Autapomorphies: 59: 1; 165: 1; apomorphies: 14: 1; 81: 1; 102: 3; 153: 1; 162: 1; 163: 1; 164: 1.

Asilinae. Autapomorphies: 170: 2; 206: 0; apomorphies: 49: 1; 55: 1; 64: 1; 168: 2; 183: 1; 214: 2.

Laphriinae. Autapomorphy: 42: 1; apomorphies: 85: 1; 172: 5; 197: 0.

Dioctriinae. Autapomorphy: 113: 2; apomorphies: 14: 2; 19: 1; 53: 1; 79: 2; 118: 2; 154: 1; 184: 1; 197: 0: 211: 1.

Trigonomiminae. Autapomorphy: 44: 1; apomorphies: 74: 1; 88: 0; 90: 0; 182: 1; 201: 1; 218: 0.

Stichopogoninae. Autapomorphy: 64: 2; apomorphies: 14: 2; 28: 1; 48: 1; 122: 0; 143: 1; 170: 6; 185: 2.

Molecular-only analyses

The parsimony analysis of the entire, combined molecular data set in POY resulted in a single most parsimonious tree (Fig. 5) of cost 25,793 under iterative pass optimization (CI = 0.20 and RI = 0.49 with uninformative characters excluded; 25,913 under direct optimization). The implied alignment for this topology can be downloaded as a whole from the TreeBase website (study accession number: S2293; matrix accession number: M4352) and as a whole as well as separately for each gene from: http://www.tdvia.de/research/research_data.html.

Asilidae is monophyletic, as are 4 of the 12 subfamily taxa (Fig. 5, Table 3). The clade Apioceridae plus Mydidae forms the sister taxon to Asilidae. Evaluating the DNA sequence data, 31 autapomorphic changes (18S = 7, 28S = 5, *AATS* = 3, *CAD* = 7, *EF-1α* = 9) and 39 apomorphic changes (18S = 5, 28S = 9, *AATS* = 5, *CAD* = 12, *EF-1α* = 8) are unambiguously optimized at the root of Asilidae. The extended sequence lengths are as follows: 18S = 2485 bp; 28S = 4177 bp; *AATS* = 560 bp; *CAD* = 1445 bp without intron (1616 bp with intron; Fig. 1); *EF-1α* = 1027 bp without introns (1556 bp with introns; Fig. 1). The overall length of the implied alignment is 9694 bp without introns, of which 2271 bp are parsimony informative and 7423 bp are parsimony uninformative (10,394 bp with introns, 2339 bp informative, 8055 bp uninformative).

Introns in protein-encoding genes

In this study, a single spliceosomal intron was observed in *CAD* (intron 4a, position 837), and four introns were found in *EF-1α* (2a, position 412; 3a, position 588; 3b, position 738; 3c, position 1002), based on an alignment of sequences and the splicing
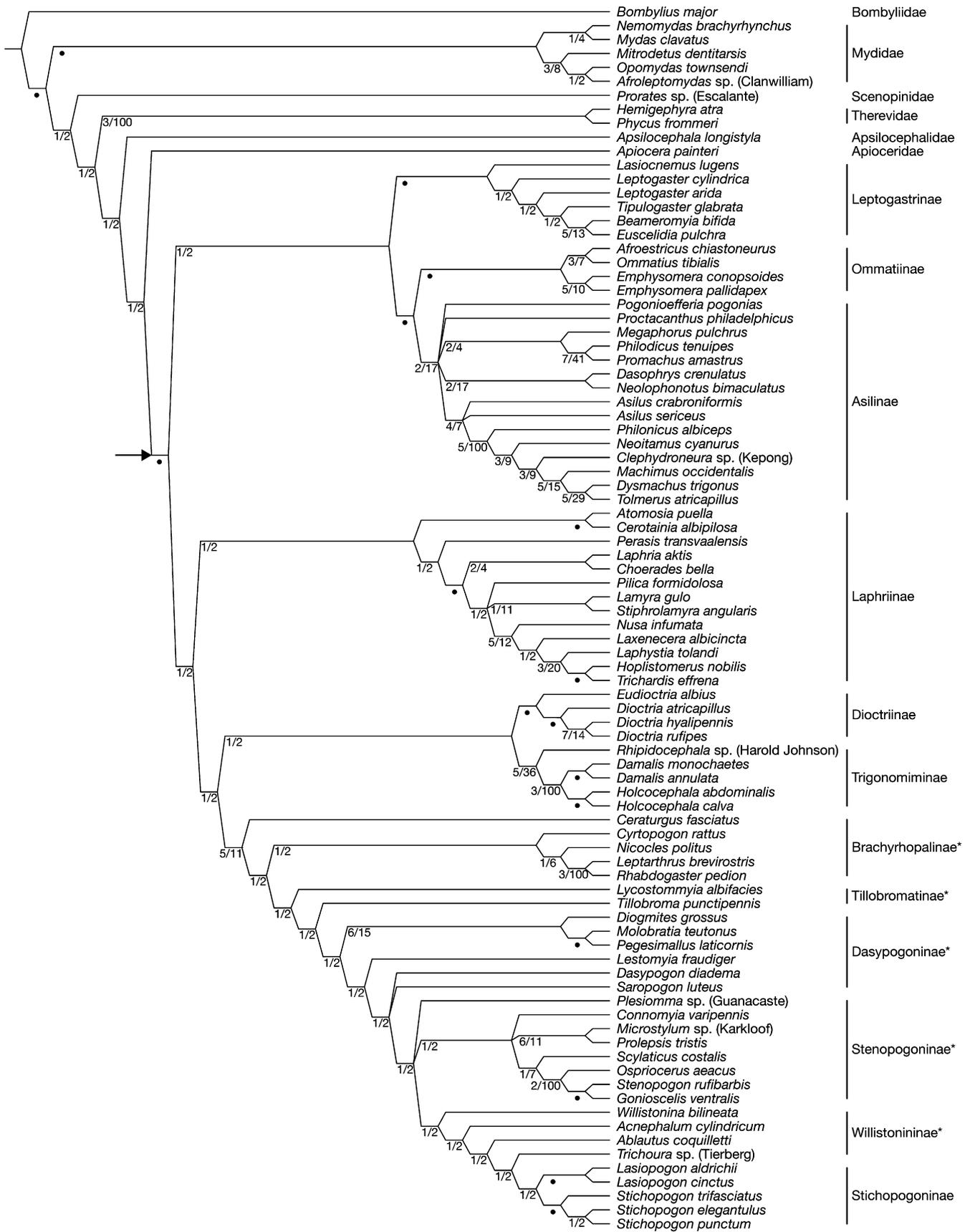
Fig. 4. Strict consensus of 18 most parsimonious cladograms from equally weighted analysis of morphology-only data in TNT (length = 1625; CI = 0.21; RI = 0.65). Bremer support/relative Bremer support shown below branches (solid circles: values ≥8/100). Arrow indicates root of Asilidae. Asterisks (*) mark non-monophyletic subfamily taxa.
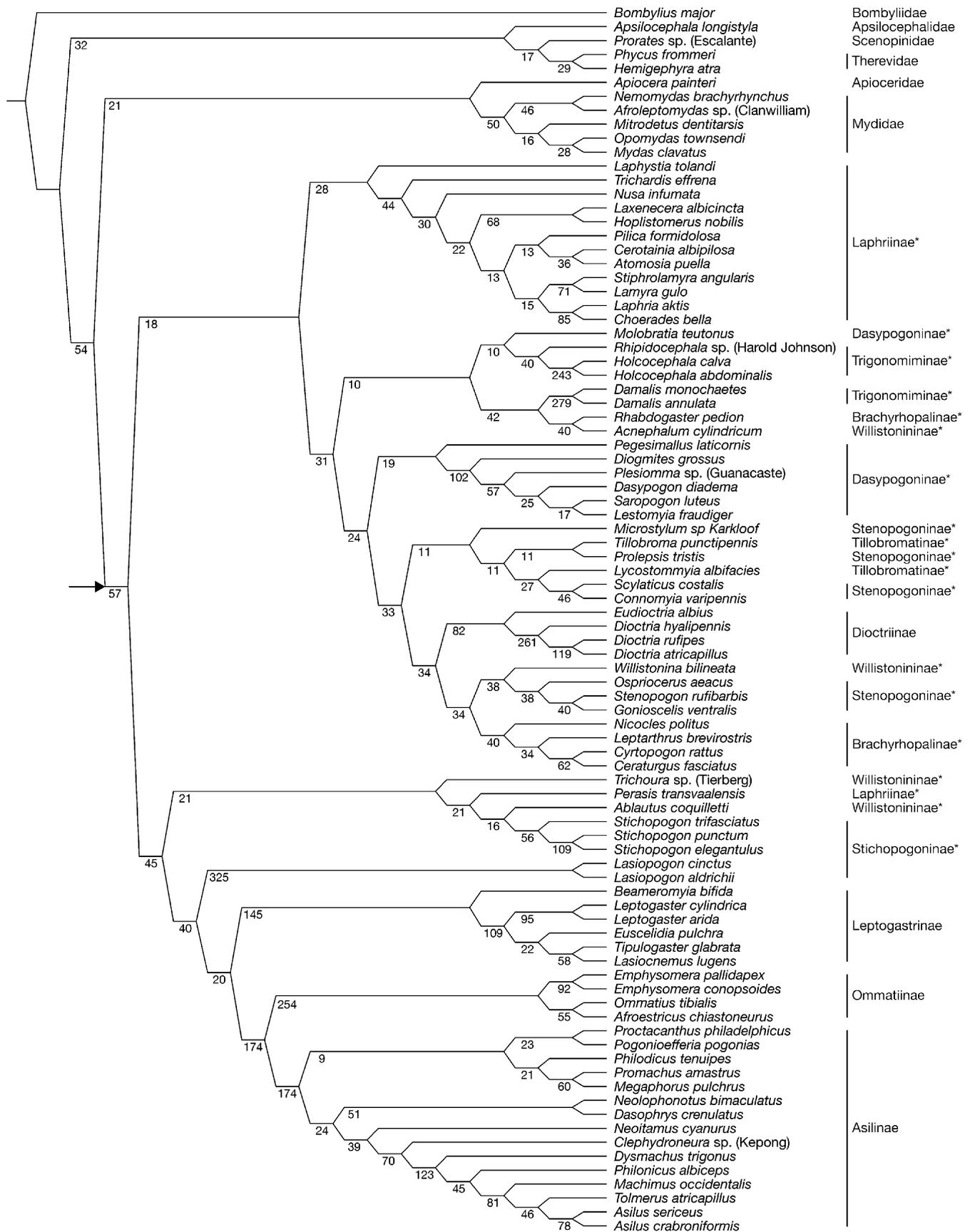
Fig. 5. Most parsimonious cladogram (25,793 steps; CI = 0.20; RI = 0.49) from equally weighted analysis of molecular-only data in POY. Bremer support values below branches. Arrow indicates root of Asilidae. Asterisks (*) mark non-monophyletic subfamily taxa.

donor/acceptor sequences GT/AG, respectively (Fig. 1, Table 5). The four introns in *EF-1α* are particularly widespread in Asilidae. A single Asilinae species exhibits an intron at position 412 (Fig. 1, Table 5; intron 2a); 33 species possess an intron of varying length at position 588 (Fig. 1, Table 5; intron 3a); five species exhibit an intron at position 738 (Fig. 1, Table 5; intron 3b); and three species possess an intron at position 1002 (Fig. 1, Table 5; intron 3c). Intron 3a is found in the following taxa that have been sequenced for the third fragment of *EF-1α* (see also Table 5 and Appendix 1): all Dasypogoninae (six species), Dioctriinae (three species),

Leptogastrinae (five species), Stichopogoninae (four species), and Mydidae (two species). Introns 3b and 3c are present in *Leptarthrus brevirostris* (Brachyrhopalinae) as well as in both included Therevidae species.

Moulton and Wiegmann (2004) found four introns in fragments 4 and 5 of *CAD* in Atelestidae, Dolichopodidae, and Hybotidae (Diptera: Eremoneura: Empidoidea). Judging from an alignment of combined data sets (data not shown, available from author), none of those introns is homologous to the one found in fragment 4 of the single Asilinae species (Fig. 1, Table 5; intron 4a, position 837). Djernæs and Damgaard (2006) have

Table 5. Spliceosomal introns found within protein-encoding genes *CAD* and *EF-1α* (see also Fig. 1).

Family-group taxon	Species	*CAD* 4a	*EF-1α* 2a	*EF-1α* 3a	*EF-1α* 3b	*EF-1α* 3c
Asilinae	*Pogonioefferia pogonias*	171	–	–	–	–
Asilinae	*Neoitamus cyanurus*	–	113	–	–	–
Brachyrhopalinae	*Cyrtopogon rattus*	–	–	55	–	–
Brachyrhopalinae	*Ceraturgus fasciatus*	–	–	61	–	–
Brachyrhopalinae	*Leptarthrus brevirostris*	–	–	–	58	59
Dasypogoninae*	*Dasypogon diadema*	–	–	60	–	–
Dasypogoninae*	*Diogmites grossus*	–	–	69	–	–
Dasypogoninae*	*Molobratia teutonus*	–	–	50	–	–
Dasypogoninae*	*Pegesimallus laticornis*	–	–	59	–	–
Dasypogoninae*	*Saropogon luteus*	–	–	57	–	–
Dioctriinae*	*Dioctria hyalipennis*	–	–	53	–	–
Dioctriinae*	*Dioctria rufipes*	–	–	59	–	–
Dioctriinae*	*Eudioctria albius*	–	–	59	–	–
Laphriinae	*Hoplistomerus nobilis*	–	–	115	–	–
Laphriinae	*Laphria aktis*	–	–	71	–	–
Laphriinae	*Laphystia tolandi*	–	–	–	64	–
Laphriinae	*Laxenecera albicincta*	–	–	105	–	–
Leptogastrinae*	*Beameromyia bifida*	–	–	63	–	–
Leptogastrinae*	*Lasiocnemus lugens*	–	–	64	–	–
Leptogastrinae*	*Leptogaster cylindrica*	–	–	62	–	–
Leptogastrinae*	*Leptogaster arida*	–	–	65	–	–
Leptogastrinae*	*Euscelidia pulchra*	–	–	63	–	–
Leptogastrinae*	*Tipulogaster glabrata*	–	–	59	–	–
Stenopogoninae	*Connomyia varipennis*	–	–	60	–	–
Stenopogoninae	*Gonioscelis ventralis*	–	–	60	–	–
Stenopogoninae	*Microstylum* sp. (Karkloof)	–	–	57	–	–
Stenopogoninae	*Plesiomma* sp. (Guanacaste)	–	–	56	–	–
Stenopogoninae	*Prolepsis tristis*	–	–	–	63	–
Stenopogoninae	*Scylaticus costalis*	–	–	57	–	–
Stichopogoninae*	*Lasiopogon aldrichii*	–	–	64	–	–
Stichopogoninae*	*Lasiopogon cinctus*	–	–	64	–	–
Stichopogoninae*	*Stichopogon punctum*	–	–	95	–	–
Stichopogoninae*	*Stichopogon trifasciatus*	–	–	74	–	–
Tillobromatinae	*Lycostommyia albifacies*	–	–	54	–	–
Trigonomiminae	*Rhipidocephala* sp. (Harold Johnson)	–	–	70	–	–
Willistonininae	*Willistonina bilineata*	–	–	54	–	–
Mydidae*	*Mitrodetus dentitarsis*	–	–	56	–	–
Mydidae*	*Opomydas townsendi*	–	–	53	–	–
Therevidae*	*Hemigephyra atra*	–	–	–	50	79
Therevidae*	*Phycus frommeri*	–	–	–	57	65

Species ordered by family-group taxon; *: all sequenced species possess the respective intron (see also Appendix 1).
Numbers indicate respective intron length in bp.

reviewed the presence of introns in *EF-1α* in Hexapoda. Brady and Danforth (2003) proposed the presence of an intron within the F1 copy of *EF-1α* in Colletidae (Hymenoptera: Apoidea) supporting the monophyly of this taxon. Within Asiloidea, Yang et al. (2000) found an intron within *EF-1α* in three Therevidae species (of the 33 sequenced species), one Bombyliidae, and a single Scenopinidae species. Judging from an alignment of combined data sets (data not shown, available from author), none of the introns found within *EF-1α* is homologous to the intron of the F1 copy of Colletidae (Brady and Danforth 2003), nor to the intron found by Yang et al. (2000) in Therevidae.

The presence of these introns, therefore, might be of phylogenetic significance and informative in future phylogenetic studies of subordinate taxa in Asilidae.

Discussion

Monophyly of and relationships among higher-level taxa

The Asilinae, Dioctriinae, Laphriinae, Leptogastrinae, Ommatiinae, and Stichopogoninae are recovered as monophyletic, as previously hypothesized by Dikow (2009), and are supported by a number of autapomorphic character states (see Results, Fig. 3, Table 4).

Most surprisingly, however, this total evidence analysis does not recover the monophyly of Trigonomiminae (Figs. 2, 3). This subfamily taxon was proposed by Papavero (1973) based on the 'goggle-eyed' appearance and the enlarged anterior tentorial pits on the head. Dikow (2009) postulated monophyly as supported by a single autapomorphy, i.e. anterior tentorial pits well-developed and conspicuous antero-ventrally (character 44: 1), and by additional apomorphic character states, i.e. apex of labella pointed (24: 1), postocular setae consisting of regular setae without macrosetae (66: 1), prosternum and proepisternum fused, prosternum narrow above prothoracic coxa (74: 1), supra-alar setae absent (90: 0), female spermathecae occupying more than posterior three abdominal segments (182: 1). Trigonomiminae is supported as monophyletic in the present morphology-only analysis, with the following suite of character changes: autapomorphic: 44: 1, apomorphic: 74: 1; 88: 0, 90: 0; 182: 0; 201: 1; 218: 0 (Fig. 4). In contrast in the total evidence analysis, a clade comprising the two included species of *Holcocephala* Jaennicke, 1867 plus *Rhipidocephala* sp. (Harold Johnson) forms the sister group to the remaining Asilidae, whereas the two species of *Damalis* Fabricius, 1805 group with *Acnephalum cylindricum* and *Rhabdogaster pedion* in a different position in the cladogram. The resulting non-monophyly of

Trigonomiminae cannot be attributed to poor taxon sampling or lack of data, as all corresponding species are represented with a more or less complete data set and only sequences for *EF-1α* are missing in some instances (see Appendix 1). Furthermore, the homology statements made for the morphological character states delimiting Trigonomiminae by Dikow (2009) are all plausible, as all of them are easily observed and assigned to discrete states, e.g. supra-alar setae either present or absent and female spermathecae occupying either the last two abdominal segments or the entire abdomen. Evaluating the number of character states optimized for these genera highlights the fact that all of these clades have many molecular autapomorphic and apomorphic character changes (Fig. 3, Table 4). These flies are not only morphologically distinct from other robber flies, but also the nuclear loci sequenced here suggest a high evolutionary rate of base changes compared to other clades.

No fossil species of Trigonomiminae has been reported to date. The minimum age of this taxon – assuming its monophyly – can be estimated, however, based on the phylogenetic hypothesis by Dikow (2009). Trigonomiminae was placed as the sister taxon to Leptogastrinae in that study, and the oldest fossil assigned to the latter taxon by Dikow (2009) is 90 million years old, from New Jersey amber (Grimaldi and Cumming 1999). Therefore, morphological and molecular evolution of this clade dates back to the late Cretaceous. It appears as if the morphological characters hypothesized to delimit a monophyletic Trigonomiminae (Dikow 2009; present morphology-only analysis, see Fig. 4) developed prior to rapid molecular divergence or are more conserved than the DNA sequences obtained for the present study. The species representing Trigonomiminae included here are distributed in the USA (*Holcocephala* species) and South Africa (*Damalis* and *Rhipidocephala* Hermann, 1926 species), respectively. Adding additional species from a broader geographical range in future total evidence analyses will help determining the monophyly or non-monophyly of Trigonomiminae as presently delimited.

Interestingly, *Plesiomma* sp. (Guanacaste) groups within the Dasypogoninae (except *Molobratia teutonus*) in the total-evidence (Fig. 2) and molecular-only analyses (Fig. 5) – in contrast to results from exclusively morphological analyses (Dikow 2009; present morphology-only analysis, see Fig. 4). The most obvious apomorphic feature of Dasypogoninae as delimited by Dikow (2009) is the large, straight spine on the prothoracic tibia (character 106); this spine is absent in *Plesiomma* sp. (Guanacaste). The optimization of this character on the total-evidence (Figs. 2, 3) and the molecular-only cladograms (Fig. 5) indicates that the spine evolved in the most recent common ancestor of Dasypogoninae and separately in *Molobratia*

teutonus, and has been reduced once in *Plesiomma* sp. (Guanacaste). Reduction of this spine has occurred independently in *Archilestris magnificus* (Walker, 1854), which is not included in the present study but grouped within Dasypogoninae in the morphological analysis by Dikow (2009). *Molobratia teutonus* has almost always been associated with Dasypogoninae (Hull 1962; Papavero 1973; Geller-Grimm 2004; Dikow 2009); only Lehr (1999) grouped the genus *Molobratia* in Dioctriinae. The position of *Plesiomma* Macquart, 1838 needs to be addressed in future studies including more morphological and DNA sequence data, as two different hypotheses of its phylogenetic relationships currently exist: (1) within Stenopogoninae sensu Dikow (2009) based on morphology; (2) within Dasypogoninae based on combined morphological and DNA sequence data in the present analysis.

Clade A (31 species; Figs. 2, 3) represents that part of the cladogram in which a number of hypotheses of phylogenetic relationships proposed by Dikow (2009) are contradicted. The included species were assigned to Stenopogoninae (21 species), Trigonomiminae (2 *Damalis* species), and Dasypogoninae (8 species) by Papavero (1973) and Geller-Grimm (2004). Dikow (2009) divided the Stenopogoninae sensu Papavero (1973) and Geller-Grimm (2004) into six subfamily taxa to recognize strictly monophyletic taxa. Four of the latter are represented here (Brachyrhopalinae, Stenopogoninae, Tillobromatinae, and Willistonininae). Although all of the species representing these taxa are placed within Clade A, none of the subfamily taxa is recovered as monophyletic in the present combined analysis (Figs. 2, 3; Table 3). Brachyrhopalinae is non-monophyletic with respect to *Rhabdogaster pedion*, Stenopogoninae (sensu Dikow 2009) is divided in three clades, the two included Tillobromatinae do not form a clade, and the four Willistonininae species form three separate clades. Clade B (a subclade within Clade A) comprises the Stenopogoninae sensu Dikow (2009) as well as Dioctriinae, Tillobromatinae, and one Willistonininae species. As clades A and B comprise species formerly assigned to Stenopogoninae sensu Papavero (1973) and Geller-Grimm (2004) (plus *Damalis*, Dasypogoninae, and Dioctriinae), one could argue that these authors' classification should be accepted. That this cannot be done, however, is exemplified by the lack of any morphological or molecular autapomorphy for either clade (Fig. 3, Table 4) and by the relatively low number of apomorphic character changes (Clade A: morphology 74: 3, 114: 2, 202: 0, 217: 0; 18S = 1, 28S = 2, *AATS* = 3, *CAD* = 13, *EF-1α* = 1. Clade B: morphology 14: 2; 28S = 1, *AATS* = 6, *CAD* = 8, *EF-1α* = 6; see also Table 4). The morphological hypothesis by Dikow (2009) supports each of the four subfamily taxa with a unique set of apomorphic character states; future research needs to target these

taxa to evaluate their monophyly (see also Conclusions below).

Tillobromatinae is a biogeographically interesting taxon that is restricted to the southern hemisphere. It is represented in the present study by *Lycostommyia albifacies* from South Africa and *Tillobroma punctipennis* from Chile, but its monophyly, supported in the morphological study by Dikow (2009), could not be confirmed.

The Brachyrhopalinae, represented by five species, is not monophyletic due to the placement of *Rhabdogaster pedion* outside of a clade comprising the other four species (Figs. 2, 3). Dikow (2009) postulated that the small S-shaped spur on the prothoracic tibia found in *Leptarthrus brevirostris* and *Nicocles politus* (Brachyrhopalinae) is not homologous to the large spine found in Dasypogoninae (character 106). This hypothesis is corroborated by molecular data here, as *L. brevirostris* and *N. politus* do not group in Dasypogoninae sensu Dikow (2009).

Bybee et al. (2004) published the only molecular phylogenetic study on Asilidae to date; its findings were reviewed by Dikow (2009). Comparing the present total evidence hypothesis to Bybee et al.'s parsimony results (their Fig. 3), the following remarks can be made. (1) Leptogastrinae is shown here to be positioned deeply within Asilidae, rather than as the sister taxon to the remaining Asilidae. (2) Asilinae includes Apocleinae sensu Papavero (1973) in the present analysis, because Apocleinae is found to be non-monophyletic. (3) Laphriinae here includes *Laphystia* Loew, 1847, which is not more closely related to *Ospriocerus* Loew, 1866 and *Stenopogon* Loew, 1847 than to any other Laphriinae. (4) Asilidae is the sister taxon to a clade composed of Apioceridae plus Mydidae in the present analysis, rather than to the remaining Asiloidea except Bombyliidae as hypothesized by Bybee et al. (2004). It appears that the latter study's limited taxon sampling of 26 robber fly species was insufficient to both test the monophyly of higher-level taxa and propose a hypothesis of higher-level relationships within Asilidae. Not even the extended taxon and character sampling in the present study can provide unambiguous evidence for the interrelationships of all subfamily taxa. The most striking feature of Bybee et al.'s parsimony hypothesis is the position of Leptogastrinae as the adelphotaxon to the remaining Asilidae, which had been postulated before by Martin (1968) based on morphological comparisons and had led him to erect a separate family-group taxon for these morphologically distinct assassin flies. Bybee et al. (2004, p. 795) stated: "Overall, the basal placement of Leptogastrinae appears to be well supported via molecular data, with nearly 47% of the signal originating from 16S rDNA, whereas the other genes provide positive but lower support values." The mitochondrial 16S rDNA, which has a length of approximately 600 bp, was not sequenced for the present study. Thus, it is an open question whether this gene

would provide the same signal with an expanded taxon sampling, or whether it would outweigh the other genetic markers, which place Leptogastrinae deeply within Asilidae, as it did in Bybee et al. (2004). Dikow's (2009) morphological hypothesis and the present total evidence approach position the Leptogastrinae deeply within Asilidae, and there is neither morphological nor molecular evidence contradicting this placement, although the sister taxon to Leptogastrinae has not been resolved (see below).

That Laphriinae is the sister taxon to the remaining Asilidae, as postulated by Dikow (2009), could not be corroborated. However, the presently hypothesized placement of a clade *Holcocephala* plus *Rhipidocephala* in this position (Fig. 2) is not strongly supported (see above). As the clade Apioceridae plus Mydidae has been corroborated as the adelphotaxon of Asilidae, the morphological characters discussed to support the position of Laphriinae as the sister taxon to the remaining Asilidae by Dikow (2009) can still be considered as valid. *Holcocephala* and *Rhipidocephala* species do not share any of these features and exhibit the apomorphic character states, whereas all Apioceridae, Laphriinae, and Mydidae exhibit the plesiomorphic character states, i.e. prothoracic and mesothoracic coxae oriented posteriorly (character 109), and male epandrium and hypandrium separated (201) (see Dikow 2009).

In contrast to the morphological hypothesis by Dikow (2009), in the present analysis Leptogastrinae is the adelphotaxon of a clade composed of Asilinae plus Ommatiinae, with these two clades combining to form the sister taxon to Stichopogoninae (Fig. 2). Leptogastrinae was postulated to be sister to Trigonomiminae by Dikow (2009), and the adelphotaxon to their combined clade was Dioctriinae. The Asilinae and Ommatiinae were positioned as the sister group to the remaining Asilidae except Laphriinae. Comparing the morphological hypothesis of the higher-level relationships within Asilidae by Dikow (2009) and the present analysis, it becomes apparent that there is no consensus on the placement of most subfamily taxa. It can be postulated that Laphriinae is the adelphotaxon to the remaining Asilidae, and that Asilinae and Ommatiinae form a clade. Furthermore, Leptogastrinae is placed deeply within Asilidae, contrary to the hypothesis that it is the adelphotaxon to Asilidae (Martin 1968; Bybee et al. 2004).

Phylogenetic relationships within higher-level taxa

As the present total evidence hypothesis is based on fewer taxa than the detailed morphological study (Dikow 2009), the monophyly of many tribal taxa cannot be tested.

The relationships within Asilinae are much more resolved in the present combined analysis than from morphological characters alone, as anticipated by Dikow (2009). Apocleini, with *Megaphorus pulchrus*, *Philodicus tenuipes*, and *Promachus amastrus*, is the only tribal taxon represented by more than one species, and is recovered as monophyletic. A separation of Asilinae into Apocleinae and Asilinae sensu stricto, as proposed by Papavero (1973), would not recognize monophyletic taxa, because the 'Apocleinae' genera *Dasophrys* Loew, 1858, *Megaphorus* Bigot, 1857, *Neolophonotus* Engel, 1925 (see Londt 2004), *Philodicus* Loew, 1847, *Pogonioefferia* Artigas and Papavero, 1997, *Proctacanthus* Macquart, 1838, and *Promachus* Loew, 1858 do not form a clade. The delimitation of Asilinae as proposed by Hull (1962), Artigas and Papavero (1997), and Dikow (2009) is therefore corroborated in the present analysis.

Within Laphriinae, the Atomosiini, Ctenotini, Hoplistomerini, and Laphriini are each represented by more than one species and are supported as monophyletic, with the exception of Hoplistomerini. This latter taxon, which comprises *Hoplistomerus nobilis* and *Trichardis effrena*, was supported as monophyletic with six apomorphic character states in the morphological study (Dikow 2009), but is here found to be non-monophyletic. The phylogenetic relationships among Laphriinae genera are very similar to those proposed by Dikow (2009) in that Andrenosomatini, Atomosiini, Ctenotini, and Laphriini form a clade in a derived position, whereas *Perasis transvaalensis* is shown to be the sister taxon to the remaining Laphriinae.

Lasiopogon Loew, 1847 is supported as adelphotaxon to the remaining Stichopogoninae as proposed by Cannings (2002) and Dikow (2009).

Within Leptogastrinae, the hypothesis that a clade comprising *Beameromyia* Martin, 1857 and *Euscelidia* Westwood, 1850 is the sister group to the remaining Leptogastrinae (Dikow 2009) is corroborated. *Lasiocnemus lugens* groups with *Tipulogaster glabrata*, in contrast to the morphological hypothesis by Dikow (2009), and therefore renders the genus *Leptogaster* Meigen, 1803 monophyletic. However, this should not be taken as evidence for the monophyly of the speciose *Leptogaster*, as the two included species from the Nearctic and western Palaearctic regions belong to *Leptogaster* sensu stricto. A detailed study of Leptogastrinae is being prepared by the author.

Comparison of separate and combined analyses

All three hypotheses presented here (Figs. 2, 4, 5) include different sets of data; consequently, the different costs/lengths of the phylogenetic hypotheses derived

from parsimony analysis do not allow one hypothesis to be favored over another. In the present study, the matrix with the fewest characters, i.e. morphology, exhibits the lowest cost. As outlined in the introduction, the total evidence hypothesis including all available data presently available for Asilidae is the most informative phylogenetic hypothesis presented here (Fig. 2). Differences in topology among the three hypotheses should not come as a surprise, as morphological and DNA sequence data might carry very different phylogenetic signals. The strength of simultaneously analyzing several data sources is exactly the combination of different signals, as well as the emerging 'secondary signal' (Nixon and Carpenter 1996). As far as we know, the coded morphological characters and genetic loci used here are linked neither by developmental pathways nor by other epigenetic interactions. The aim of comparing the total evidence hypothesis to the morphology-only and molecular-only results merely is to indicate the different signals that morphological and molecular data might provide, as well as to analyze whether the molecular data outcompete the information provided by the fewer morphological characters.

One concern often voiced by morphologists is that the large number of molecular characters will outcompete the relatively fewer morphological characters in a phylogenetic study; this is the reason why combining morphological and molecular data is not always practiced. That the number of characters is actually not that different is exemplified by evaluating the respective numbers of parsimony informative characters: morphology = 211 (95.9%); DNA in total evidence = 2367 (22.8%; 18S = 358, 28S = 620, $AATS = 238$, $CAD = 686$, $EF\text{-}1\alpha = 465$); DNA in molecular-only = 2339 (22.5%; 18S = 354, 28S = 608, $AATS = 236$, $CAD = 686$, $EF\text{-}1\alpha = 455$). Although the number of parsimony informative characters from DNA sequences is about ten times higher than from morphology, it is much reduced (by a factor of five) relative to the total sequence data. Using only the autapomorphies it becomes apparent that some taxa are supported entirely by morphological characters, others entirely by molecular ones (Fig. 3, Table 4). For example, the Laphriinae possess two morphological autapomorphies, but not a single molecular autapomorphic character change is optimized for this clade in the total evidence analysis (Fig. 3). This taxon is found to be non-monophyletic in the molecular-only analysis, due to the placement of *Perasis transvaalensis* in a separate position, but it is monophyletic in the total-evidence and morphology-only analyses. It appears that the two characters of the postocciput and the abdominal tergites in male Laphriinae provide strong morphological evidence for the monophyly of this taxon, whereas it is the molecular data that provide information on the relationships within Laphriinae, as they are identical in

the molecular-only and total-evidence analyses but very different in the morphology-only analysis (Figs. 2–5).

Another example with a different pattern is given by the morphologically easily distinguished Ommatiinae, in which all species possess setae on the anterior surface of the antennal stylus (character 59). Although monophyletic in all three analyses, it is only supported as such by two morphological autapomorphies in the total-evidence and morphology-only analyses (Fig. 3). In contrast, 24 molecular autapomorphies are optimized at the root in both the total-evidence and molecular-only analyses (Table 4), which strengthens the evidence for the monophyly of this taxon.

Trigonomiminae shows yet another pattern in that it is monophyletic in the morphology-only analysis, but non-monophyletic in the total-evidence and molecular-only analyses (see also above, and Table 3). The separate position of *Holcocephala* plus *Rhipidocephala* and *Damalis* in the total evidence hypothesis cannot necessarily be attributed to the molecular data outcompeting the morphological data. This is because the five Trigonomiminae species are placed in a relatively small clade of eight species together with *Acnephalum cylindricum*, *Molobratia teutonus*, and *Rhabdogaster pedion* in the molecular-only analysis, a grouping supported by only a single molecular autapomorphy in *CAD* and by 20 apomorphies (18S = 4, 28S = 4, $AATS = 4$, $CAD = 6$, $EF\text{-}1\alpha = 2$). This 8-taxon clade is not present in the total evidence analysis; thus one has to conclude that the morphological data provide a certain signal that contradicts the molecular signal, but in the presence of molecular data is not strong enough to group all Trigonomiminae species in a single clade.

Low phylogenetic resolution within the morphologically very similar Asilinae has been found in previous morphological studies (Dikow 2009), and is also found to some degree in the present morphology-only analysis (Fig. 4). The addition of DNA sequence data enhanced the resolution and provided character support for the majority of clades within Asilinae (Figs. 3, 6). In addition, the phylogenetic relationships among Asilinae are identical in the total-evidence and molecular-only analyses, suggesting that the molecular data provide a stronger signal than the few morphological characters that are informative within this clade.

A total evidence analysis with several data partitions provides the opportunity to examine the character support provided by the individual characters within the partitions. As not all character transformations in molecular data can be visualized and incorporated into a scientific publication, one clade is selected as an example. The character support for clades within Asilinae (Fig. 6) illustrates that a mixture of character state transformations within the morphological and molecular data is responsible for the grouping of species. The majority of autapomorphies stem from the 18S and
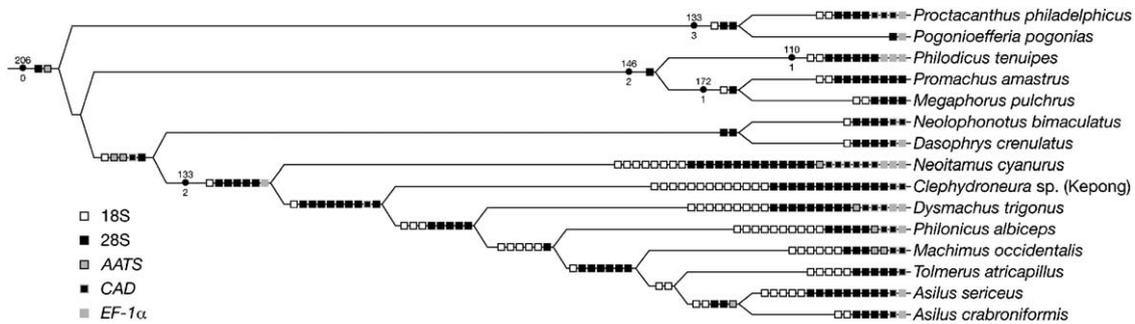
Fig. 6. Phylogenetic relationships among Asilinae inferred from total evidence analysis (Fig. 2), with character optimization and distribution mapped onto cladogram (unambiguous optimization). Solid circles on branches represent morphological autapomorphies, with respective character number shown above and character state below. Squares indicate molecular autapomorphies for each gene separately.

Table 6. Monophyly evaluations for Asilidae subfamily taxa (see Dikow 2009) from present total evidence analysis (Fig. 2), Bybee et al. (2004, their Fig. 3), and two previous studies.

Subfamily taxon	Present study	Bybee et al. (2004)	Geller-Grimm (2004)	Papavero (1973)
Asilinae	•	Apo + Asi	Apo + Asi	Apo + Asi
Bathypogoninae	/	/	in Ste	in Ste
Brachyrhopalinae	–	1	in Das, Ste	in Das, Ste
Dasypogoninae	–	–	–	–
Dioctriinae	•	/	•	in Ste
Laphriinae	•	Lar + 1 Lay	Lar + Lay	Lar + Lay
Leptogastrinae	•	•	•	/
Ommatiinae	•	1	•	•
Phellinae	/	1	in Ste	in Ste
Stenopogoninae	–	–	–	–
Stichopogoninae	•	1	•	in Ste
Tillobromatinae	–	1	in Ste	in Ste
Trigonomiminae	–	1	•	•
Willistonininae	–	/	in Ste	in Ste

Symbols: • = monophyletic; – = non-monophyletic; / = no representative included; 1 = based on a single species.
Taxon abbreviations: Apo = Apocleinae; Asi = Asilinae; Das = Dasypogoninae; Lar = Laphriinae; Lay = Laphystiinae; Ste = Stenopogoninae.

28S ribosomal DNA, although nine autapomorphies are also provided by *AATS*, which has only 238 parsimony informative sites overall. It appears that no single gene is entirely responsible for the character support for either relationships among the higher-level taxa within Asilidae or relationships within these higher-level taxa (Fig. 6, Table 4). It is a mixture of morphological and molecular data that is informative, and future studies can only improve our understanding of the phylogenetic relationships within Asilidae by employing more comprehensive taxon sampling or adding more data.

Conclusions

The present phylogenetic hypothesis is based on the largest amount of data – 7300 bp of nuclear DNA and 211 morphological characters for 77 species – assembled on Asilidae to date. The taxon sampling is somewhat limited in comparison to the morphological study by Dikow (2009), which included 158 assassin-fly species. Not only are the biogeographically interesting Australian and Chilean Bathypogoninae and Phellinae not represented, but other crucial species (of Brachyrhopalinae, Stenopogoninae, Tillobromatinae, and Willistonininae) are also not included because of the lack of specimens preserved for DNA extraction. Tillobromatinae and Willistonininae are taxa with disjunct distribution in South America plus southern Africa and North America plus Africa, respectively, and were only recently separated from Stenopogoninae in the sense of previous authors by Dikow (2009). Testing the monophyly of the included taxa will require exhaustive sampling on all continents. Brachyrhopalinae was also newly proposed (Dikow 2009) and is currently the least understood subfamily taxon, as most species are relatively small and

exhibit very generalized morphology. However, four of the five included species form a clade.

A total evidence analysis is the most comprehensive summary of data and knowledge (e.g. Grant and Kluge 2003). However, from the point of taxon representation the present study lacks too many species; therefore no formal, new classification is derived from the cladogram in Fig. 2. What the present extensive analysis highlights, though, are those taxa that need to be addressed in future phylogenetic studies. Some taxa, e.g. Leptogastrinae and Ommatiinae, have always been regarded as monophyletic (Table 6). On the other hand, the Dasypogoninae and Stenopogoninae sensu previous authors have been divided into several monophyletic taxa by Dikow (2009) (Table 6), who also noted that these taxa will need to be addressed in much more detail than Ommatiinae, for example. Even after exploring many new morphological character systems and sequencing some 7300 base pairs of nuclear DNA, we are still far away from reaching a consensus on the higher-level phylogenetic relationships within Asilidae. What cannot be disputed is the monophyly of the speciose Asilidae. Future phylogenetic analyses should be based on the general framework provided by Dikow (2009) plus the present total evidence hypothesis, and will need to include more species particularly for clade A (Fig. 2), as well as for three clades sensu Dikow (2009, Fig. 120), i.e. clade F, Brachyrhopalinae, and Willistonininae. I suggest that both morphological and molecular data need to be explored further to decipher the phylogenetic relationships of the main lineages within Asilidae.

Acknowledgments

Appendix A. Supplementary material

Supplementary data (Appendix 1; five sequence data files) associated with this study can be found in the online edition at doi:10.1016/j.ode.2009.02.004.

References

Artigas, J.N., Papavero, N., 1997. The American genera of Asilidae (Diptera): keys for identification with an atlas of female spermathecae and other morphological details. IX. 1. Subfamily Asilinae Leach (including Apocleinae Lehr): key to generic groups. Arq. Zool. 34, 57–63.

Brady, S.G., Danforth, B.N., 2003. Recent intron gain in Elongation Factor-1α of colletid bees (Hymenoptera: Colletidae). Mol. Biol. Evol. 21, 691–696.

Bremer, K., 1988. The limits of amino acid sequence data in angiosperm phylogenetic reconstruction. Evolution 42, 795–803.

Bremer, K., 1994. Branch support and tree stability. Cladistics 10, 295–304.

Bybee, S.M., Taylor, S.D., Nelson, C.R., Whiting, M.F., 2004. A phylogeny of robber flies (Diptera: Asilidae) at the subfamilial level: molecular evidence. Mol. Phyl. Evol. 30, 789–797.

Cannings, R.A., 2002. The Systematics of Lasiopogon (Diptera: Asilidae). Royal British Columbia Museum, Victoria.

Collins, K.P., Wiegmann, B.M., 2002. Phylogenetic relationships and placement of the Empidoidea (Diptera: Brachycera) based on 28S rDNA and EF-1α sequences. Insect Syst. Evol. 33, 421–444.

Danforth, B.N., Lin, C.-P., Fang, J., 2005. How do insect nuclear ribosomal genes compare to protein-coding genes in phylogenetic utility and nucleotide substitution rate? Syst. Entomol. 30, 549–562.

Danforth, B.N., Sauquet, H., Packer, L., 1999. Phylogeny of the bee genus Halictus (Hymenoptera: Halictidae) based on parsimony and likelihood analyses of nuclear EF-1alpha sequence data. Mol. Phyl. Evol. 13, 605–618.

Dikow, T., 2004. Family-group names in the Asilidae (Diptera). Studia Dipterol 10, 459–471.

Dikow, T., 2009. Phylogeny of Asilidae inferred from morphological characters of imagines (Insecta: Diptera: Brachycera: Asiloidea). Bull. Am. Mus. Nat. Hist. 319, 1–175.

Djernæs, M., Damgaard, J., 2006. Exon-intron structure, paralogy and sequenced regions of Elongation Factor-1 alpha in Hexapoda. Arthropod Syst. Phyl. 64, 45–52.

Edgar, R.C., 2004. Muscle: multiple sequence alignment with high accuracy and high throughput. Nucleic Acids Res. 32, 1792–1797.

Freudenstein, J.V., Pickett, K.M., Simmons, M.P., Wenzel, J.W., 2003. From basepairs to birdsongs: phylogenetic data in the age of genomics. Cladistics 19, 333–347.

Friedlander, T.P., Regier, J.C., Mitter, C., 1992. Nuclear gene sequences for higher level phylogenetic analysis: 14 promising candidates. Syst. Biol. 41, 483–490.

Galtier, N., Gouy, M., Gautier, C., 1996. SeaView and Phylo_win, two graphic tools for sequence alignment and molecular phylogeny. Comput. Appl. Biosci. 12, 543–548.

Geller-Grimm, F., 2004. World catalogue of the genera of the family Asilidae (Diptera). Studia Dipterol 10, 473–526.

Giribet, G., 2001. Exploring the behavior of POY, a program for direct optimization of molecular data. Cladistics 17, S60–S70.

Giribet, G., Carranza, S., Baguñà, J., Riutort, M., Ribera, C., 1996. First molecular evidence for the existence of a Tardigrada + Arthropoda clade. Mol. Biol. Evol. 13, 76–84.

Goloboff, P.A., 1999. Analysing large data sets in reasonable times: solutions for composite optima. Cladistics 15, 415–428.

Goloboff, P.A., Farris, J.S., 2001. Methods for quick consensus estimation. Cladistics 17, S26–S34.

Goloboff, P.A., Farris, J.S., Nixon, K.C., 2008. TNT – Tree Search Using New Technologies (version 1.1, December 2007). TNT, a free program for phylogenetic analysis. Cladistics 24, 774–786. (available at http://www.zmuc.dk/public/phylogeny/TNT).

Grant, T., Kluge, A.G., 2003. Data exploration in phylogenetic inference: scientific, heuristic, or neither. Cladistics 19, 379–418.

Grimaldi, D., 1990. Diptera. In: Grimaldi, D. (Ed.), Insects from the Santana Formation, Lower Cretaceous, of Brazil. Bull. Am. Mus. Nat. Hist. 195, 164–183.

Grimaldi, D., Cumming, J., 1999. Brachyceran Diptera in Cretaceous ambers and Mesozoic diversification of the Eremoneura. Bull. Am. Mus. Nat. Hist. 239, 1–124.

Grimaldi, D., Engel, M.S., 2005. Evolution of the Insects. Cambridge University Press, Cambridge, MA.

Hennig, W., 1973. Diptera (Zweiflügler). In: Helmcke, J.G., Starck, D., Wermuth, H. (Eds.), Handbuch der Zoologie. Eine Naturgeschichte der Stämme des Tierreichs. IV. Band, 2. Hälfte, 2. Teil, No. 31. De Gruyter, Berlin.

Holston, K.C., Irwin, M.E., Wiegmann, B.M., 2007. Monophyly and phylogenetic relationships of Thereva and therevine genus-groups (Insecta: Diptera: Therevidae) based on EF-1α, 28S rDNA and mitochondrial 16S rDNA sequences. Invert. Syst. 21, 279–296.

Hull, F.M., 1962. Robber flies of the world. Bull. United States Nat. Mus. 224, 1–907.

Karl, E., 1959. Vergleichend-morphologische Untersuchungen der männlichen Kopulationsorgane bei Asiliden. Beitr. Entomol. 9, 619–680.

Kluge, A.G., 1989. A concern for evidence and a phylogenetic hypothesis of relationships among Epicrates (Boidae, Serpentes). Syst. Zool. 38, 7–25.

Kluge, A.G., Wolf, A.J., 1993. Cladistics: What's in a word? Cladistics 9, 183–199.

Lee, C.-H., Satô, M., Shepard, W.D., Jäch, M., 2007. Phylogeny of Psephenidae (Coleoptera: Byrrhoidea) based on larval, pupal and adult characters. Syst. Entomol. 32, 502–538.

Lehr, P.A., 1999. Asilidae. In: Lehr, P.A. (Ed.), Key to the Insects of the Russian Far East. Vol. 6, Diptera and Siphonaptera. Part I. Dal'nauka, Vladivostok, pp. 591–640.

Londt, J.G.H., 2004. The status of *Neolophonotus* Engel, 1929 and *Megadrillus* Bigot, 1857 within the Afrotropical asilid fauna (Diptera: Asilidae: Apocleinae). Studia Dipterol. 10, 393–394.

Malia, M.J., Lipscomb, D.L., Allard, M.W., 2003. The misleading effects of composite taxa in supermatrices. Mol. Phyl. Evol. 27, 522–527.

Martin, C.H., 1968. The new family Leptogastridae (the grass flies) compared with the Asilidae (robber flies) (Diptera). J. Kans. Entomol. Soc. 41, 70–100.

Miller, K.B., Bergsten, J., Whiting, M.F., 2007. Phylogeny and classification of diving beetles in the tribe Cybistrini (Coleoptera, Dytiscidae, Dytiscinae). Zool. Scr. 36, 41–59.

Moulton, J.K., 2003. Can the current molecular arsenal adequately track rapid divergence events within Simuliidae (Diptera)? Mol. Phyl. Evol. 27, 45–57.

Moulton, J.K., Wiegmann, B.M., 2004. Evolution and phylogenetic utility of *CAD* (*rudimentary*) among Mesozoic-aged Eremoneuran Diptera (Insecta). Mol. Phyl. Evol. 31, 363–378.

Moulton, J.K., Wiegmann, B.M., 2007. The phylogenetic relationships of flies in the superfamily Empidoidea (Insecta: Diptera). Mol. Phyl. Evol. 43, 701–713.

Nixon, K.C., 1999. The parsimony ratchet, a new method for rapid parsimony analysis. Cladistics 15, 407–414.

Nixon, K.C., 2002. WinClada (version 1.00.08). Program distributed by the author. Cornell University, Ithaca, NY.

Nixon, K.C., Carpenter, J.M., 1996. On simultaneous analysis. Cladistics 12, 221–241.

Noll, F.B., 2002. Behavioural phylogeny of corbiculate Apidae (Hymenoptera; Apinae), with special reference to social behaviour. Cladistics 18, 137–153.

Papavero, N., 1973. Studies of Asilidae (Diptera) systematics and evolution. I. A preliminary classification in subfamilies. Arq. Zool. 23, 217–274.

Robillard, T., Legendre, F., Desutter-Grandcolas, L., Grandcolas, P., 2006. Phylogenetic analysis and alignment of behavioural sequences by direct optimization. Cladistics 22, 602–619.

Varón, A., Vinh, L.S., Bomash, I., Wheeler, W.C., 2008. POY 4.0.2870. American Museum of Natural History, New York (available at http://research.amnh.org/scicomp/projects/poy.php).

Wenzel, J.W., 1992. Behavioural homology and phylogeny. Annu. Rev. Ecol. Syst. 23, 361–381.

Wheeler, W.C., 1996. Optimization alignment: the end of multiple sequence alignment in phylogenetics? Cladistics 12, 1–9.

Wheeler, W.C., 2003. Iterative pass optimization. Cladistics 19, 254–260.

Whiting, M.F., 2002. Mecoptera is paraphyletic: multiple genes and phylogeny of Mecoptera and Siphonaptera. Zool. Scr. 31, 93–104.

Wiegmann, B.M., Tsaur, S.-C., Webb, D.W., Yeates, D.K., Cassel, B.K., 2000. Monophyly and relationships of the Tabanomorpha (Diptera: Brachycera) based on 28S ribosomal gene sequences. Ann. Entomol. Soc. Am. 93, 1031–1038.

Winterton, S.L., Wiegmann, B.M., Schlinger, E.I., 2007. Phylogeny and Bayesian divergence time estimations of small-headed flies (Diptera: Acroceridae) using multiple molecular markers. Mol. Phyl. Evol. 43, 808–832.

Woodley, N.E., 1989. Phylogeny and classification of the 'orthorrhaphous' Brachycera. In: McAlpine, J.F., Wood, D.M. (Eds.), Manual of Nearctic Diptera, vol. 3. Agriculture Canada Res. Branch Monogr. 32; Hull, Quebec.

Yang, L., Wiegmann, B.M., Yeates, D.K., Irwin, M.E., 2000. Higher-level phylogeny of the Therevidae (Diptera: Insecta) based on 28S ribosomal and Elongation Factor-1alpha gene sequences. Mol. Phyl. Evol. 15, 440–451.

Yeates, D.K., 1994. The cladistics and classification of the Bombyliidae (Diptera: Asiloidea). Bull. Am. Mus. Nat. Hist. 219, 1–191.

Yeates, D.K., 2002. Relationships of extant lower Brachycera (Diptera): a quantitative synthesis of morphological characters. Zool. Scr. 31, 105–121.

Yeates, D.K., Irwin, M.E., 1996. Apioceridae (Insecta: Diptera): cladistic reappraisal and biogeography. Zool. J. Linn. Soc. 116, 247–301.